



**ADDIS ABABA INSTITUTE OF TECHNOLOGY**

**SCHOOL OF GRADUATE STUDIES**

**SCHOOL OF CIVIL AND ENVIRONMENTAL ENGINEERING**

**” Use of DCP and CBR Tests to Characterize Subgrade Shear Strength”**

**The Case of Volcanic Ash/Pyroclastic Deposit of Bulbula - Alage Section**

**By: Yohannes Woldechirkos**

A THESIS SUBMITTED TO THE SCHOOL OF GRADUATE STUDIES, ADDIS ABABA UNIVERSITY, IN PARTIAL FULFILLMENT OF THE REQUIREMENTS FOR THE DEGREE OF MASTERS OF SCIENCE IN CIVIL ENGINEERING [GEOTECHNICAL ENGINEERING]

**Advisor: Dr.-Ing. Tensay Gebremedhin**

April, 2023

School of Graduate Studies  
School of Civil and Environmental Engineering

**Use of DCP and CBR Tests to Characterize Subgrade Shear  
Strength**

By: Yohannes Woldechirkos

Thesis Submitted to School of Graduate Studies in Partial Fulfillment of the  
Requirement for Degree of Master of Science in Geotechnical Engineering

**Approved by Board of Examiners**

<u>Dr.-Ing. Tensay Gebremedhin</u>	_____	_____
Advisor	signature	Date
<u>Dr.-Ing. Henok Fikre</u>	_____	_____
Internal Examiner	signature	Date
<u>Dr.-Ing. Asrat Worku</u>	_____	_____
External Examiner	signature	Date
_____	_____	_____
Chairman	signature	Date

## **Declaration**

I, the undersigned, declare that this thesis is my original work performed under the supervision of my research advisor **Dr.-Ing. Tensay Gebremedhin** and has not been presented as a thesis for a degree in any other university. All sources of materials used for this thesis have been duly acknowledged.

Name: YOHANNES WOLDECHIRKOS

Signature: \_\_\_\_\_

Place Institute of Technology

Addis Ababa University

Addis Ababa.

Date: \_\_\_\_\_

**ACKNOWLEDGMENT**

Great glory goes to the ALMIGHTY GOD “all things are from Him to Him”, who is always standing at the right of my side in each and every step of my life.

I wish to express my deepest gratitude to my advisor Dr. Tensay Gebremedhin for his invaluable guidance and advice to the realization of the thesis. He sacrificed his time, resource and provided me all necessary information to carry out the research.

My special thanks also go to Beza Consulting Engineers central laboratory, Lidet Consulting Engineers central laboratory and Bulbula – Alage road project material department staff for providing me every access to their laboratories and performing the tests with me without any hesitation.

My sincere thank goes to my family, whose commitment to the work and their vision makes this research possible.

### ABSTRACT

The existing manuals adopted in Ethiopia for road construction and management purpose have made CBR and/or DCP tests mandatory in order to characterize strength of unbounded materials. Executing CBR and DCP tests is obligatory that, the data is available easily in every road stretch throughout the country. Contrary to this, the shear strength parameters used in slope stability analyses and bearing capacity computations are not available in sufficient number. For this reason, this research is initiated with the objective of obtaining values of shear strength parameters of pyroclastic/volcanic ash deposits using CBR and/or DCP test results on a pilot study area Bulbula – Alage road section. Different test results of Atterberg limit, sieve analysis, proctor, California bearing ratio, direct shear, dynamic cone penetration, field density, collapsibility and dispersity tests have been used. According to the test results, the plasticity of subgrade is low to none; the sand fraction is significant; the maximum dry density of the deposit is mainly below  $1.5 \text{ g/cm}^3$ ; the deposit has high CBR and low CBR swell values; DCP penetration rate decreases with depth in the majority of the stretch. The level of collapsibility potential is moderate with dispersity potential ranging from none to moderate.

For this non-plastic to low plastic, low dry density, high CBR and moderate collapsible potential pyroclastic deposit a correlation is developed between CBR and/or DCP test results with that of angle of internal friction value obtained from direct shear test. The correlating equation has been developed using Excel and SPSS statistical analysis software.

**TABLE OF CONTENTS**

**ACKNOWLEDGMENT..... I**

**ABSTRACT .....II**

**TABLE OF CONTENTS..... III**

**LIST OF TABLES ..... VI**

**LIST OF FIGURES ..... VII**

**LIST OF SYMBLOS AND ABBREVIATIONS ..... VIII**

**CHAPTER 1 INTRODUCTION..... 1**

1.1 Background..... 1

1.2 Objectives ..... 2

1.2.1 General objective..... 2

1.2.2 Specific objectives..... 3

1.3 Research Methodology ..... 3

**CHAPTER 2 LITERATURE REVIEW ..... 5**

2.1 Pyroclastic Deposit ..... 5

2.1.1 Relationship to Topography ..... 5

2.1.2 Structures and Textures in Unwelded Pyroclastic Deposits..... 6

2.1.3 Engineering Properties of Pyroclastic Deposit..... 6

2.2 Dynamic Cone Penetrometer Test..... 7

2.2.1 DCP Testing ..... 7

2.2.2 Applications ..... 8

2.2.3 Limitations of a DCP Test..... 9

2.3 California Bearing Ratio..... 9

2.3.1 CBR Testing ..... 9

2.3.2 Why CBR Test is Easily Available ..... 10

2.3.3 Effect of Density on CBR values ..... 10

2.4 Shear strength ..... 11

2.4.1 Direct Shear Strength Testing Method..... 11

2.4.2 Shear Strength of Cohesionless Soils..... 11

2.5	Correlation between DCP Test and Unconfined Compressive Strength.....	13
2.6	Correlation between DCP and CBR Value .....	14
2.7	Correlation between CBR and Shear Strength Parameters .....	14
<b>CHAPTER 3 METHODOLOGY .....</b>		<b>17</b>
3.1	General.....	17
3.2	Sampling Area Description .....	17
3.2.1	Topography .....	17
3.2.2	Climate .....	18
3.2.3	Geological Setting .....	19
3.3	Field Investigation .....	21
3.3.1	Subgrade Soil Investigations.....	21
3.3.2	Reconnaissance Soil Survey.....	21
3.3.3	Subgrade Material Sampling and Testing .....	23
3.3.4	Dynamic Cone Penetrometer Test (DCP Testing) .....	26
3.3.5	In-Situ Density Test .....	27
<b>CHAPTER 4 ANALYSIS OF FIELD AND LABORATORY TEST RESULTS.....</b>		<b>29</b>
4.1	Introduction .....	29
4.2	Laboratory Test Results.....	29
4.2.1	Atterberg Limit.....	29
4.2.2	Particle Size Analysis.....	31
4.2.3	Soil Classification .....	32
4.2.4	Evaluation of Collapsibility of the Soil.....	33
4.2.5	Evaluation of Dispersiveness of the Subgrade.....	34
4.2.6	Moisture – Density Relationship.....	36
4.2.7	California Bearing Ratio (CBR).....	39
4.2.8	Direct Shear Test.....	41
4.3	Field Test Results .....	43
4.3.1	Field Density Test .....	43
4.3.2	Dynamic Cone Penetrometer .....	44
4.4	Comparison between Field and Laboratory Test Results.....	46

4.4.1	Field and Laboratory Dry Densities and Moisture Content .....	46
4.4.2	CBR Value at Field and Laboratory Dry Densities.....	48
<b>CHAPTER 5 CORRELATION BETWEEN CBR/DCP AND SHEAR STRENGTH PARAMETERS 50</b>		
5.1	General.....	50
5.2	Regression Analysis .....	50
5.3	Correlation between DCP and CBR Values .....	52
5.4	Modeling Shear Strength Parameters Using DCP or CBR Value .....	53
<b>CHAPTER 6 CONCLUSION AND RECOMMENDATION .....</b>		<b>55</b>
6.1	Conclusion .....	55
6.2	Recommendation .....	56
<b>REFERENCES .....</b>		<b>57</b>
<b>APPENDIX .....</b>		<b>60</b>

**LIST OF TABLES**

Table 3-1: Terrain Classification.....	17
Table 3-2: Basic Climatic Data of the Project Area (Alage Area).....	19
Table 3-3: Geological Formation .....	20
Table 3-4: Soil Extension Survey.....	22
Table 4-1: Collapse Potential Test Result .....	34
Table 4-2: Chemical Test Result.....	34
Table 4-3: Double Hydrometer Test Result .....	36
Table 4-4: Maximum Dry Density and Optimum Moisture Content of the Subgrade .....	37
Table 4-5: CBR and CBR Swell Values of the Subgrade .....	40
Table 4-6: Direct Shear Values of the Subgrade.....	42
Table 4-7: Field Density by Sand Replacement Method .....	43
Table 4-8: Weighted Average DCPI Values .....	45
Table 4-9: Field and Laboratory Dry Density and Moisture Content Values .....	46
Table 4-10: CBR Value at MDD and Field Dry Density Values.....	48
Table 5-1: Statistical Measure between DCPI and CBR Correlation .....	52
Table 5-2: Statistical Summary for the Correlation .....	54

**LIST OF FIGURES**

Figure 2-1: DCP Instrument (Simon, D., and Piouslin, S., 2006).....8

Figure 2-2: Direct Shear Test Result in Loose, Medium, and Dense Sands (M.Das, 1997).. 12

Figure 2-3: Peak and Ultimate Friction Angles from the Direct Shear Test (M.Das, 1997) .13

Figure 2-4: Comparison Between Correlated CBR and Laboratory CBR Values (Gregory, G., and Cross, S., 2007)..... 16

Figure 2-5: Unsaturated Shear Strength Vs CBR for Sand (Purwana, M., and Nikraz, H., 2014)..... 16

Figure 3-1: Location of the Pilot Route Corridor..... 18

Figure 3-2: Geological Formation (Mengesha, T., et al, 1996) ..... 20

Figure 3-3: Pyroclastic Deposit.....23

Figure 3-4: Excavated Test Pits ..... 24

Figure 3-5: DCP Test .....26

Figure 3-6: Field Density by Sand Replacement Method (on the Upper and Lower Layer).28

Figure 4-1: Variation of Plasticity Index (%) of the Subgrade soils.....30

Figure 4-2: Plasticity Chart of the Subgrade Soil (ISC/UCS).....30

Figure 4-3: Particle Size Distribution of Subgrade Soils along the Road Alignment.....32

Figure 4-4: Percentage Compositions of Soil Classification .....33

Figure 4-5: Cations Composition in the Soil.....35

Figure 4-6: Maximum Dry Density of the Tested Pits.....37

Figure 4-7: Optimum Moisture Content of the Tested Pits.....38

Figure 4-8: Maximum Dry Density (Proctor Test Undertaken During Bulbula – Alage Road Construction).....38

Figure 4-9: CBR Value of the Tested Pits.....40

Figure 4-10: CBR Swell Value of the Tested Pits .....40

Figure 4-11: CBR Value (CBR Test Undertaken During Bulbula – Alage Road Construction).....41

Figure 4-12: Dry Density of the Tested Pits .....44

Figure 4-13: Rate of Penetration Value of the Tested Pits.....46

Figure 4-14: Laboratory MDD versus Field Dry Density values.....47

Figure 4-15: Comparison of CBR Value at In-Situ Dry Density and 95% of MDD Value...49

Figure 5-1: Correlation/Scatter Plot Between Angle of Internal Friction and DCPI Values.53

Figure 5-2: Correlation/Scatter Plot Between Angle of Internal Friction and DCPI Values.54

**LIST OF SYMBOLS AND ABBREVIATIONS**

AASHTO	American Association of State Highway and Transportation officials
ASTM	American Society for Testing and Materials
c	cohesion
Ca <sup>++</sup>	Calcium Ion
CBR	California Bearing Ratio
CEC	Cation Exchange Capacity
cm	Centimeter
Cu	Undrained Cohesive Resistance
DCP	Dynamic Cone Penetrometer
DCPI	Dynamic Cone Penetrometer Index
ECDSWC	Ethiopia Construction Design and Supervision Works Corporation
ERA	Ethiopian Roads Administration
ESP	Exchangeable Sodium Percentage
ISC	Indian Soil Classification
K <sup>++</sup>	Potassium
Km	Kilometer
kPa	Kilo Pascal
LL	Liquid Limit
Na <sup>++</sup>	Sodium Ion
NNE-SSW	North to North East – South to South West
m	Meter

## Use of DCP and CBR tests to Characterize Subgrade Shear Strength

---

mm	Millimeter
MER	Main Ethiopian Rift
MDD	Maximum Dry Density
Mg <sup>++</sup>	Magnesium Ion
OMC	Optimum Moisture Content
$\phi$	Angle of internal friction
PI	Plasticity Index
PL	Plastic Limit
SPSS	Statistical Package for the Social Sciences
TRL	Transport Research Laboratory
UCS	Unconfined Compression Strength
USC	Unified Soil Classification

## CHAPTER 1 INTRODUCTION

### 1.1 Background

All road projects in Ethiopia use California Bearing Ratio (CBR) as a measure to determine strength of subgrade, subbase and base course materials. Ethiopian Road Administration (ERA) use CBR as a measure for evaluating strength of the subgrade. In order to characterize in-situ strength of the subgrade material, dynamic cone penetration (DCP) test is used and is correlated with CBR value. Therefore, as a result of requirements in the existing Ethiopian Road Administration Manual plenty of CBR and DCP test results of Ethiopian soil are available.

In road construction projects of Ethiopia, CBR and DCP tests are undertaken within 1 km interval during the design stage and the testing interval is intensive during construction stage especially for the CBR test. But shear strength tests are undertaken only during construction stage, in foundation investigation of bridge structures for span greater than 10 m. As a result of this, shear strength parameters required for slope stability analysis and bearing capacity calculation of structures (especially for minor drainage structures) are not available easily. Therefore, if strong correlation is developed between the available CBR and/or DCP tests and rarely undertaken shear strength test, shear strength parameters will easily be estimated from the correlation. And also, since we do have plenty of CBR and DCP data available from each road project, we will have the corresponding shear strength parameters from the correlation.

The ASTM D1883 and AASHTO T193 laboratory test technique for the CBR test compare the resistance to penetration of the test specimen to that of a "standard" sample of well-graded crushed stone material using a standard-sized piston. As a result of its simplicity and existing road administration manuals of Ethiopia most consultants are equipped with CBR testing machines.

DCP test is a portable and simple device which is used to measure the material's in-situ resistance to penetration. As a result of its simplicity and adopted by ERA manual for measuring in-situ performance of the subgrade, its being used to characterize in-situ strength of the subgrade. The test can be extended with an extension rod.

On this thesis work, the direct shear test results were correlated with the CBR and/or DCP test result outputs. A direct shear test determines a soil's shear strength by forcing it to shear

at a constant rate along an induced horizontal axis of weakness. The sample was consolidated using three distinct weights and then sheared at the same constant rate in at least three subtests. Each subtest's peak and residual shear stress were measured and graphed. Using this data, cohesion and friction angle of the soil were determined.

Direct shear test is used to predict cohesion and friction angle quickly, especially in cohesionless soils. In cohesionless soils, the drainage is quick and pore pressure dissipates very rapidly that for conducting drained tests on cohesionless soils, direct shear test is ideally suited for this.

The pyroclastic deposit has covered significant area of the Ethiopian central rift valley especially the section between Lake Zeway in the north and Lake Hawasa in the south. A pyroclastic flow/deposit is mostly of a fast-moving current of hot gas and volcanic matter that flows along the ground away from a volcano. In majority of the stretch from Zeway to Hawasa towns section, the deposit is thicker than 5 m. Pyroclastic deposit of the stated section of Ethiopian rift valley is majorly cohesionless material that shear strength parameters can be estimated with direct shear test effectively.

Significant section of the material existing in the stated stretch have low in-situ dry density value than maximum dry density (MDD). For this material, when we report CBR value of the subgrade at the maximum dry density found in the laboratory we will obtain exaggerated value.

In this research CBR value of the material will be calculated taking the dry density obtained on site. Correlation will be developed between CBR and/or DCP and direct shear test results for the sample taken from the upper and lower part of the 1.5 m deep test pit.

In addition to obtaining the shear strength parameters required for slope stability and bearing capacity computations, if correlation is developed between the CBR and/or DCP test and shear strength tests, the professional will have a strong sense/visualization for the in-situ shear strength value of the soil.

## **1.2 Objectives**

### **1.2.1 General objective**

The general objective of the thesis work is to estimate values of shear strength parameters of pyroclastic/volcanic ash deposit using CBR and/or DCP test result

### 1.2.2 Specific objectives

The specific objectives of the thesis work which will make up the general objective stated above are dictated as follows:

- To assess the variation of strength of the pyroclastic deposit with depth and compare the strength at in-situ dry density with strength attained at 95% MDD.
- To inspect chemical composition and behavior of the pyroclastic/volcanic ash deposit.
- To investigate the sensitivity level of DCP and/or CBR test with that of the shear strength parameters.

### 1.3 Research Methodology

The main sources of data for the analysis of the soil are obtained from road projects designed/constructed in the central part of the Ethiopian rift valley. The majority of test results of CBR, proctor, Atterberg limit, shear strength, sieve analysis, dispersity and collapsibility identification tests were taken from previously designed and/or constructed projects around the study area.

In order to explore lateral extent of the soil, reconnaissance soil survey was conducted along representative road segment (pilot stretch section Bulbula – Alage road segment). The soil survey along the road corridor was carried out by visual observation of color, texture, moisture and appearance of the soil along the road side and from test pits dug.

To determine the engineering properties of the soil along the Bulbula – Alage road segment, representative disturbed samples were collected from a test pit of approximately - 1.0 m x 1.0 m wide and a minimum depth of 1.5 m below the existing ground level unless rock stratum is encountered and make excavation impossible. Samples of about 60 kg were taken from each test pit for laboratory tests stated below.

- Wet Sieve analysis (AASHTO T27),
- Liquid limit (AASHTO T 89),
- Plastic limit (AASHTO T 90),
- Collapsibility identification tests (ASTM D-5333),
- Dispersity identification tests (ASTM D-4221...),
- Modified Proctor test (AASHTO T180),
- CBR test and CBR-swell (AASHTO T193) after 4 days soaking and

- Direct shear test (AASHTO T236).

The first three are index tests which indirectly expresses behavior of the material. The fourth and fifth determines collapse and deflocculation potential of soil particles respectively. The last three are density and strength identification tests.

At the test pit depths where field densities were measured, DCP tests were conducted. In-situ densities of the subgrade material was assessed by using sand replacement method approximately between 0.2 m - 0.45 m depth for the upper layers and between 1.4 m - 1.6 m depth for the lower layers in each of the test pits.

In addition to the above listed tests which took place in the pilot road, the test results that existed from previous investigation during the design and construction of the road projects in the identified area where the subgrade is pyroclastic deposit were referred and analyzed.

CBR and/or subgrade strength class of the previous investigation work is fairly similar to the results obtained in this research work. The dry density values obtained in previous work are also nearly similar to the results obtained during the research work.

The laboratory test results were compiled and analyzed. Finally, based on the analysis result, correlations were developed between CBR and/or DCP and shear strength parameter values. The correlations obtained between CBR and/or DCP test result with that of angle of internal friction are found convincing and acceptable.

## CHAPTER 2 LITERATURE REVIEW

### 2.1 Pyroclastic Deposit

A pyroclastic flow results due to volcanic eruption; it contains volcanic ash and hot gases. The deposit significantly dominates near previously erupted volcanic areas. It can move as ground-hugging flows or air-suspended plumes, depending on their densities. The solids fraction of pyroclastic currents is made up of discrete component, i.e., pumice, free crystals, and lithics, each of which is characterized by specific size, density and shape distributions. Several mechanisms, including as turbulent suspension, fluidization, cohesive or frictional matrix strength, and grain to grain interactions, keep them in place during subaerial transport, (Jacopo, T., and Danilo. M.P., 2002).

Particles are sorted according to their sizes, densities, and shapes during both regional transport and local sedimentation of pyroclastic currents, with the degree and kind of sorting depending on flow characteristics, (Jacopo, T., and Danilo. M.P., 2002).

#### 2.1.1 Relationship to Topography

The Main Ethiopian Rift (MER) is a NNE-SSW trending rift valley, 80 km wide and 700 km long, bordered by the Ethiopian Plateau to the west and the Somali Plateau to the east. Its development has been variedly interpreted, (Woldegabriel, G., et al, 1990). On the borders of the Silti-Debre Zeit Fault Zone (SDZFFZ) on the west and the Wonji Fault Belt (WFB) on the east, dense swarms of NNE-SSW trending steep normal faults stand total offsets of roughly 1500 m – 2000 m between the rift floor and the plateau, (Woldegabriel, G., et al, 1990).

Pyroclastic flows may completely drain from upper slopes and only be preserved in the lower parts of valleys, thereby becoming initially thicker away from the source. Small-volume pyroclastic flows may be restricted to valleys in locations with severe topography. Because of the momentum of flow, pyroclastic flows move down the top slopes of volcanoes, forming levees or "high water marks" and larger rock fragments on both sides of a valley or along the outside margin of a sinuous channel. Pyroclastic flows, like lahars, spread out in fan-like lobes beyond the mountain sides, (Alexander, B., et al, 2020).

### 2.1.2 Structures and Textures in Unwelded Pyroclastic Deposits

Most unwelded pyroclastic flow deposits are poorly sorted and massive, but may show subtle grading, alignment bedding or imbrication of oriented particles. In contrast, most pyroclastic surge deposits are thinner, finer-grained and better sorted than flow deposits, and wavy or cross-bedded structures may be common, (Fisher, R.V., and Schmincke, H.U., 1984).

In the textural analysis of pyroclastic flow deposits, it is important to know the relative proportions of pumice, lithics, and crystals, (Walker, G.P.L., and Croasdale, R., 1971). Because, the size distributions, sorting, and other parameters of these three subpopulations may differ for other reasons than sorting in the eruption column and during flow. For example, lithic particles can be obtained through magmatic stopping, fragmentation of the walls of a magma chamber and vent, or fragmentation of a plug or dome within the vent, and they can also be taken up from the ground during flowage. The size distribution of crystal pieces is a result of the magma's original phenocryst sizes and breakage during explosive eruptions. Furthermore, different mineral species have a variety of size ranges (e.g., feldspar vs. magnetite). Because pumice has a poor mechanical strength, it can be decreased in size during eruption and flow, resulting in a higher concentration of pumice dust in the fine-grained portion of a deposit, (Walker, G.P.L., and Croasdale, R., 1971).

### 2.1.3 Engineering Properties of Pyroclastic Deposit

Pyroclastic deposits are known to be soils with special engineering geological properties due to the particular microscopic structure of constituent fragments. As it is well known, pyroclastic materials ejected from volcanic vents whose fragmentation is due to mechanical friction or gaseous explosion during movement of lava, have a typical vesicular structure, (Esposito, L., and Guadagno, F.M., 1998).

The processes used to prepare the material for sieving have a considerable impact on the grain size distribution curve in the experiment. Pyroclastic deposits can be broken by a weak mechanical action such as that applied by human hands, which is sufficient to separate aggregates but not strong enough to break individual particles. However, for loose pyroclastic deposits, the grain size distribution of the material obtained by hand separation is often still significantly affected by the number of sieving cycles, testifying imperfect separation of aggregates, (Manuela, C., et al, 2009).

From the point of view of grading, pyroclastic deposits are gravel to sand size. In-situ dry density of the deposit in majority of the scenarios is significantly lower than the maximum dry density obtained in the laboratory. The calculated California bearing ratio value using laboratory 95% MDD is higher than the CBR value obtain using in-situ dry density value. Due to loosen nature of the deposit while undertaking dynamic cone penetration test the number of blows required to penetrate a given depth is relatively lower. On the welded pyroclastic deposits strength of the deposit is very high that it is resistant to penetration of the DCP probe, (Woldechirkos, Y., and Desaleg, K., 2020).

## 2.2 Dynamic Cone Penetrometer Test

### 2.2.1 DCP Testing

The DCP test generate data which can be analyzed to produce accurate information on in-situ subgrade layer thicknesses and strengths. Tests can be completed quickly, and test sites can be simply re-established. A typical DCP test team of 3 people may be able to carry out 20 tests in a day at a spacing of between 50 and 500 meters. DCP test can provide information of sufficient quality and quantity to enable for the estimation of pavement strength and the planning of improvement projects. DCP test results can also be used to determine the best locations for excavating test pits to acquire additional data, (Simon, D., and Piouslin, S., 2006).

A cone is attached to the bottom of a vertical rod to form the DCP. To provide a standard impact, or 'blow,' to the cone and drive it into the pavement, a hammer is repeatedly lifted and lowered upon a coupling at the rod's mid-height. Detail of the DCP instrument is shown in Figure 2-1. The depth of penetration of the cone is measured using a vertical scale next to the rod. The penetration and the number of blows is recorded on a DCP Test Data Form. The penetration per blow, the 'penetration rate', is recorded as the cone is driven into the layer and used to calculate the strength of the material through which the cone is passing. After the completion of the test, DCP is removed by gently tapping the weight upwards against the handle. A change in penetration rate implies a difference in material strength, allowing layers to be recognized and their thickness and strength estimated, (Simon, D., and Piouslin, S., 2006).

The DCP probe cannot penetrate some strong materials such as hot mix asphalt, rock beddings and/or cement treated bases. Before the test can begin, these layers must be removed and their strength evaluated in other methods, (Simon, D., and Piouslin, S., 2006).

When undertaking the DCP test on the pavement layer, the strengths of all layers can be combined and expressed into a Structural Number or the strength of each layer can also be determined. When tests are repeated along the length of the pavement, a longitudinal picture of the pavement can be created, allowing for the detection of changes in construction and condition. These changes can then be used to divide the road into uniform sections for each of which expected lifetimes can be estimated and improvements designed, (Simon, D., and Piouslin, S., 2006).

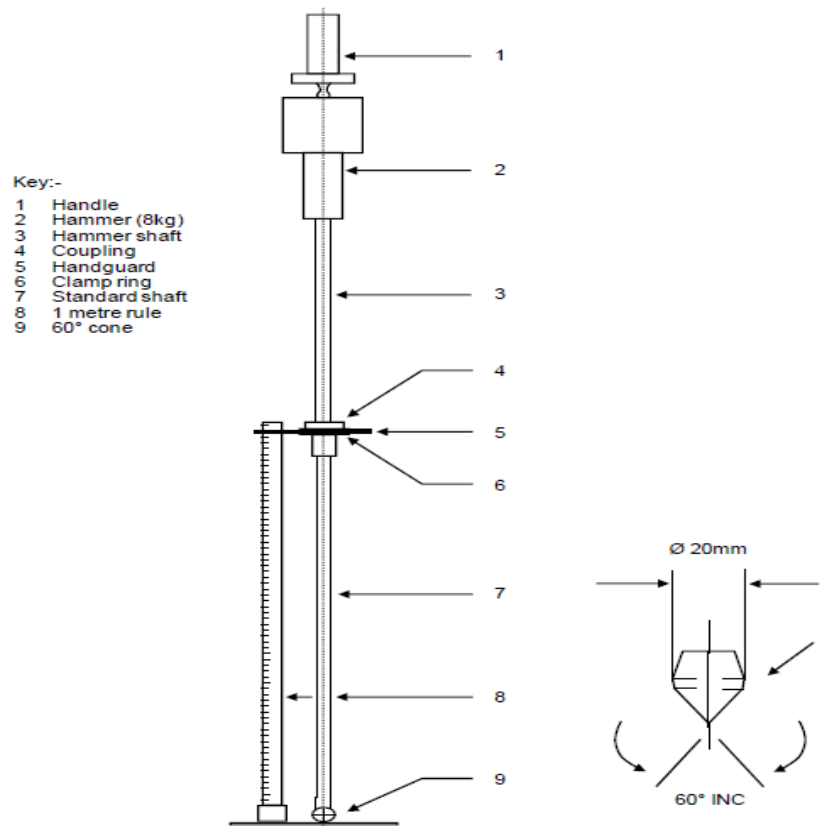


Figure 2-1: DCP Instrument (Simon, D., and Piouslin, S., 2006)

### 2.2.2 Applications

DCP testing can be used to characterize the qualities of subgrade and base materials in a variety of methods. The DCP device's biggest strength is its capacity to provide a continuous record of relative soil strength as a function of depth. By plotting a graph of rate of penetration versus depth below the testing surface, a user can observe a profile showing layer depths, thicknesses, and strength conditions. This is especially useful if the project's original as-built blueprints were lost, never prepared, or were determined to be erroneous, (Simon, D., and Piouslin, S., 2006).

The DCP's other strength lies in its small and relatively lightweight design. It can be used in restricted spaces to assess foundation settlements, such as inside structures, or on congested sites (trees, steep topography, soft soils, etc.) that would prevent larger testing equipment from being used. DCP is ideal for testing through core holes in existing pavements, (Tam, B., and Dave, J., 1993).

### **2.2.3 Limitations of a DCP Test**

This equipment is often used to evaluate material qualities below the surface to a depth of 1000 mm. Extensions rod can be used to improve the penetration depth. If extension rods are employed, however, caution should be exercised when utilizing correlations to estimate other parameters, as these correlations are only valid for certain DCP configurations. Skin friction along drive rod extensions will arise as the device's mass and inertia change, (Katie, 2019). Other limitations of the DCP test are as follows

**Surcharge Loading** - The confining pressure and accompanying surcharge loading of the pavement structure above determine the strength of a subgrade material. When DCP testing is performed, all surcharge loading is typically eliminated (i.e., in a borehole or test pit), which may not accurately reflect the in-situ strength.

**Seasonal Moisture Contents** – CBR value obtained from Dynamic Cone Penetrometer in isolation can mislead the functional CBR of the subgrade, because the seasonal moisture fluctuation may not be represented unless the test is conducted on a regular basis. Furthermore, if the pavement is flooded, the in-service moisture levels may be significantly underestimated.

## **2.3 California Bearing Ratio**

### **2.3.1 CBR Testing**

The CBR test entails compaction of a sample to a predetermined or ascertained moisture content and density using one of several standardized techniques; and penetration of the sample by a plunger at a given rate to give a specified deformation under a measured load in its existing state or after soaking. The value measured, for use in design, is the load or the resistance of the plunger to penetration. The California Bearing Ratio expresses the measured load as a percentage of the resistance obtained from a similar penetration of a reference material, (AASHTO, 2001).

### 2.3.2 Why CBR Test is Easily Available

The test is an empirical procedure that determines a soil's shear strength. This test is used frequently because it is quite simple to perform and it is widely used around the world that, there is a lot of data to help understand the results.

In 1928 and 1929, engineers at the California Division of Highways developed the CBR test to ensure pavements could be economically constructed and still carry the anticipated axle loads. They used the penetration resistance of the best crushed-rock foundation material as a comparison point for all other soil and base course materials. The CBR test was first used in California in 1935, and it is now a standard procedure in ASTM, AASHTO, Ethiopian road manuals, and other organizations. CBR values are recognized as integral to pavement and walkway design by Ethiopian road authority and Addis Ababa City Road Authority manuals. The California Bearing Ratio's reliability for pavement design has been demonstrated via extensive use over a long period of time and knowledge acquired from field correlations.

### 2.3.3 Effect of Density on CBR values

Compaction is considered as a technique for improving the engineering properties of soils, which reduces their permeability and increases their strength, (AASHTO, 2001). The California Bearing Ratio (CBR) is an important geotechnical criterion for calculating the proper thickness of flexible subgrade pavements. Because of its ramifications in transportation infrastructures construction, compaction properties and CBR are crucial. The connection between moisture content and dry density (the compaction curve) can be used to depict the compaction characteristics of soils under a particular compaction energy. The optimal moisture content and maximum dry density are represented by the abscissa and ordinate of the compaction curve's peak point, respectively. It is known that water has a dual effect of suction and lubrication; as water increases, the suction decreases. Water also lubricates particle contact, resulting in a maximum increase in dry density, (Hogentogler, J.R., 1936).

Around the maximum dry density value, a material will attain higher CBR value. A material will have a lower CBR value when the dry density is below the maximum. The relation between CBR and dry density of a given material is direct. Pyroclastic deposits have low in-situ dry density value in the natural state that, CBR value of the deposit obtained at in-situ

density is relatively lower than CBR value obtained at the maximum dry density, (Woldechirkos, Y., and Desaleg, K., 2020).

### 2.4 Shear strength

#### 2.4.1 Direct Shear Strength Testing Method

The consolidated-drained shear strength of a sandy to silty soil is determined using a direct shear test. Because shear strength is necessary whenever a structure is dependent on the soil's shearing resistance, it is one of the most significant engineering features of a soil. Shear strength is required in engineering circumstances such as estimating the stability of slopes or cuts, establishing foundation carrying capacity, and calculating the pressure applied by soil on a retaining wall, (Krishna, 2002).

The test can be performed on either undamaged or remolded samples. A soil sample can be compacted at optimum moisture content in a compaction mold to help in remolding. Then, with the right cutter, a specimen for the direct shear test may be obtained. Alternatively, the sand sample can be placed in the built shear box at the desired density. The specimen is sheared over a predetermined horizontal plane between the two halves of the shear box with a normal load applied to it. Normal displacement, shear load, and shear displacement are all measured and recorded. The test is repeated for three or more identical specimens under different normal loads. The shear strength parameters can be calculated using the results, (AASHTO, 2001).

#### 2.4.2 Shear Strength of Cohesionless Soils

For this research, a direct shear test is used to assess the shear strength of soils. The soil sample confined inside the upper and lower rigid boxes, is subjected to the normal load,  $N$  and is sheared by shear force,  $T$ . If  $A$  is the area of sheared surface, the shear stress,  $\tau$  acting on sheared surface is equal to  $T/A$ , and the normal stress,  $\sigma$ , is equal to  $N/A$ . The soil shear strength is the shear stress,  $\tau$ , that causes the soil to slip on sheared surface. It can be defined by Mohr Coulomb theory, (M.Das, 1997).

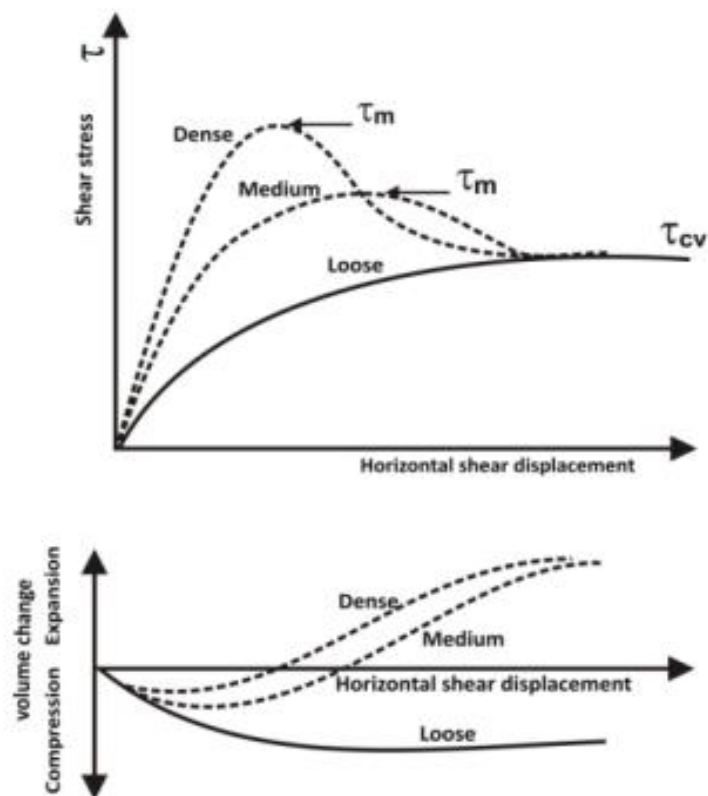


Figure 2-2: Direct Shear Test Result in Loose, Medium, and Dense Sands (M.Das, 1997)

The nature of the results of typical direct shear tests in loose, medium, and dense sands are shown in Figure 2-2. Based on Figure 2-2, the following observations can be made, (M.Das, 1997):

- i. In dense and medium sands, shear stress increases with shear displacement to a maximum or peak value,  $\tau_m$ , and then decreases to an approximately constant value,  $\tau_{cv}$ , at large shear displacements. This constant stress,  $\tau_{cv}$ , is the ultimate shear stress.
- ii. For loose sands, the shear stress increases with shear displacement to a maximum value and then remains constant.
- iii. For dense and medium sands, the volume of the specimen initially decreases and then increases with the shear displacement. At large values of shear displacement, the volume of the specimen remains approximately constant.
- iv. For loose sands, the volume of the specimen gradually decreases to a certain value and remains approximately constant thereafter

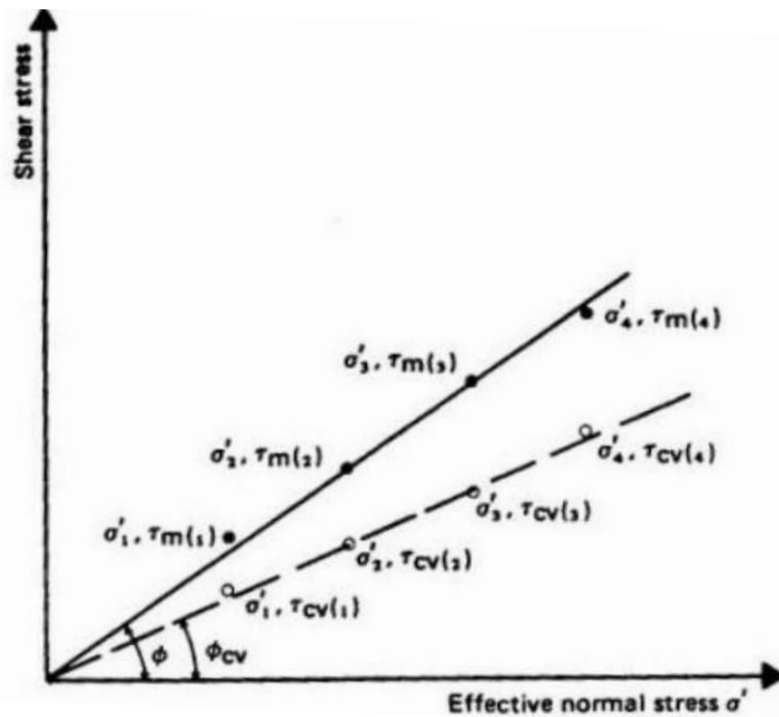


Figure 2-3: Peak and Ultimate Friction Angles from the Direct Shear Test (M.Das, 1997)

The angle of friction,  $\phi$ , for the sand can be determined by plotting a graph of the maximum or peak shear stresses vs. the corresponding normal stresses, as shown in Figure 2-3. Drawing a straight line across the origin and the points indicating the experimental outcomes yields the Mohr-Coulomb failure envelope. The slope of this line will give the peak friction angle,  $\phi$ , of the soil. Similarly, ultimate friction angle,  $\phi_{cv}$ , can be determined by plotting the ultimate shear stresses,  $\tau_{cv}$ , versus the corresponding normal stresses, as shown in Figure 2.3. The ultimate friction angle,  $\phi_{cv}$ , represents a condition of shearing at constant volume of the specimen. For loose sands, the peak friction angle is approximately equal to the ultimate friction angle, (M.Das, 1997).

## 2.5 Correlation between DCP Test and Unconfined Compressive Strength

Anteneh (2012) tried to correlate unconfined compressive strength with that of DCP test result during his study on clayey soils of Addis Ababa. He developed a model for estimating the UCS by DCPI as  $UCS = -197 \ln(DCPI) + 735.5$  with coefficient of determination  $R^2$  of 71.1% for red clay soils of Addis Ababa. Based on bearing capacity theory, this correlation was used to build a bearing capacity equation. The equation found was  $q_{ult} = -506.5 \ln(DCPI) + \gamma h + 1891$  for red clay soils of Addis Ababa.

Temnit (2014) indicated that DCPI values can be correlated to the unconfined compressive strength (UCS) of Addis Ababa Red clay soil during her research to correlate the DCP test with UCS. She took undisturbed sample and performed the unconfined compressive strength test in the laboratory and made the DCP tests on the field. She had concluded that the unconfined compression strength (UCS) is highly influenced by DCPI, bulk unit weight and natural moisture content (NMC) and liquidity Index (LI). The correlation she developed is  $UCS (kPa) = 645.70 - 115.59 \ln(DCPI)^{mm/blow} + 456.41(Liquidity\ Index, LI)$  with coefficient of determination  $R^2$  of 71.3%

### 2.6 Correlation between DCP and CBR Value

Correlations between DCP and CBR test results have been developed by different researchers. The UK DCP software developed by United Kingdom Department for International Development (DFID) have included six correlations to be used for conversion of DCP test result into CBR value, (Simon, D., and Piouslin, S., 2006) .

Yitagesu (2012) have undertaken investigation on Jimma – Bonga - Mizan, Contract 1: Jimma – Bonga road project from station 100+000 to 105+000 during his research to correlate DCP test with CBR test. On the subgrade soil, he conducted liquid limit (LL), plastic limit (PL), sieve analysis, hydrometer analysis, California bearing ratio, in-situ moisture content, and dynamic cone penetration tests. Based on this, he developed correlation to predict the CBR values of the subgrade soil from dynamic cone penetration test results. He developed correlation between CBR and DCPI values as  $\log(CBR) = 2.954 - 1.496 \log(DCPI)$  with  $R^2 = 0.943$ .

### 2.7 Correlation between CBR and Shear Strength Parameters

Black (1979) suggested the following relationship between the CBR and undrained shear strength ( $C_u$  – cohesion intercept of saturated clay), with the equation:

$$CBR = \frac{c_u}{23} \quad 2.1$$

He observed that the undisturbed over-consolidated soils failed at a much smaller strain compared to the remolded soils. The average strain to failure of undisturbed soils being only a quarter of that of remolded soils. The work of Skempton and analysis of in-situ CBR tests carried out at the laboratory indicates that in undisturbed over-consolidated soils, the stress beneath the CBR plunger at a standard penetration of 2.54 mm is normally greater than 75 %

of the stress when ultimate bearing capacity has been attained. Hence, it can be assumed that the CBR test measures the stress at the ultimate bearing capacity of undisturbed over consolidated soils. That would transform the Equation 2.1 above to be:

$$CBR = \frac{c_u}{11.5} \quad 2.2$$

Gregory and Cross (2007) investigated the correlation between shear strength of soil and CBR value by modeling piston in the CBR test as a circular foundation. The bearing capacity of the foundation on cohesive soil is directly related to its shear strength. The following correlation formulas were developed between the CBR and the ultimate bearing capacity of cohesive soils

$$CBR = \frac{q_{ult} * 100}{6895} = \frac{6.2 * C_u * 100}{6895} = 0.09C_u \quad 2.3$$

The correlation of CBR with shear strength parameters was verified by comparing correlated CBR with actual AASHTO T193 CBR results of 5 different soils. Although a limited number of soil samples were used in verification, the correlated CBR and laboratory-measured CBR values are in good agreement. The scatter plot of correlated and laboratory CBR values is shown in Figure 2-4.

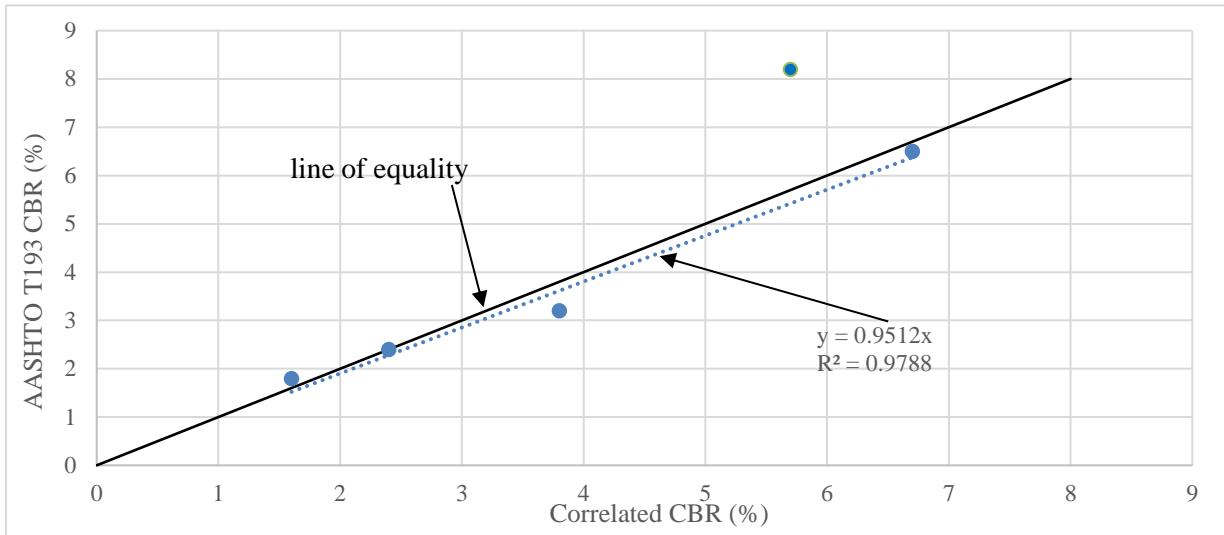


**Figure 2-4: Comparison Between Correlated CBR and Laboratory CBR Values (Gregory, G., and Cross, S., 2007)**

Purwana and Nikraz (2014) investigated the correlation between unsaturated CBR and the unsaturated shear strength of the sand-kaolin clay mixture using the suction-monitored direct shear. Suction is defined as the ability of the soil to absorb additional water, and the relationship between water content and soil suction is that the higher the soil water content, the lower suction in the soil. To monitor suction, a tensiometer was added to a traditional direct shear. The results shown in Figure 2-5 indicated that the correlation between the CBR and the unsaturated shear strength depends on the normal stress applied on the soil.

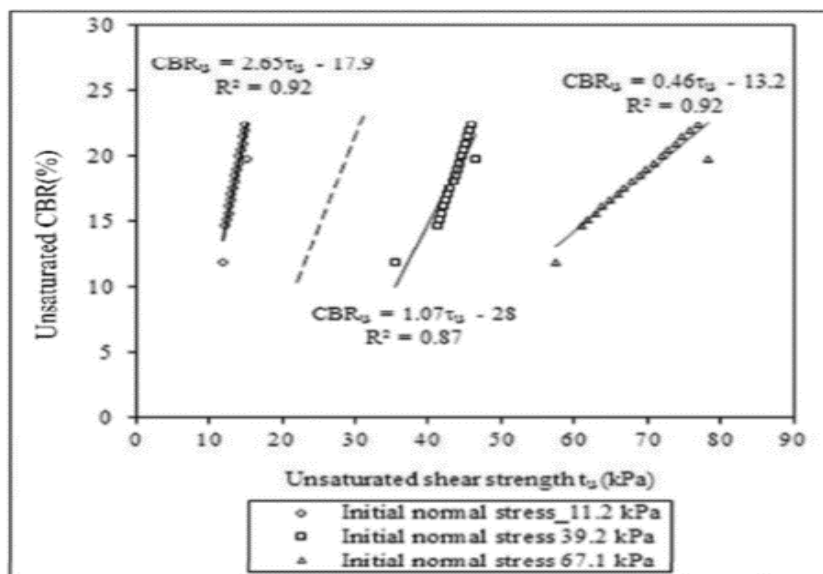


**Figure 2-5: Unsaturated Shear Strength Vs CBR for Sand (Purwana, M., and Nikraz, H., 2014)**

## CHAPTER 3 METHODOLOGY

### 3.1 General

In order to have better understanding of the pilot stretch area over-all condition in addition to undertaking field tests, climatic and topographical features of the area have been investigated. The investigation work has been undertaken taking into consideration recommendations of AAHTO, ASTM and ERA manuals. The detailed investigation work undertaken is described in the following sections.

### 3.2 Sampling Area Description

#### 3.2.1 Topography

Bulbula – Alage route corridor is located in the central part of Ethiopia. It starts 2.5 km from Bulbula town and ends at Alage, going west ward over Jiddo town. The centerline elevation rises in minor amount from station 0+000 (1605 m above sea level (A.S.L)) to station 17+800 (1641 m A.S.L) on average a rise in 2 m/km, and then it drops in a smaller amount to Alage (1600 m A.S.L) on average a fall of 3.3 m/km. The road alignment navigates majorly in flat terrain with small change in elevation. The detailed terrain classification along the route corridor is shown in Table 3-1 and location map of the pilot stretch is shown in Figure 3-1.

**Table 3-1: Terrain Classification**

No.	Station		Length (m)	Description
	From	to		
1	0+000	17+280	17280	Flat terrain
2	17+280	18+430	1150	Town section with flat terrain
3	18+430	24+660	6230	Flat terrain
4	24+660	29+100	4440	Town section with flat terrain

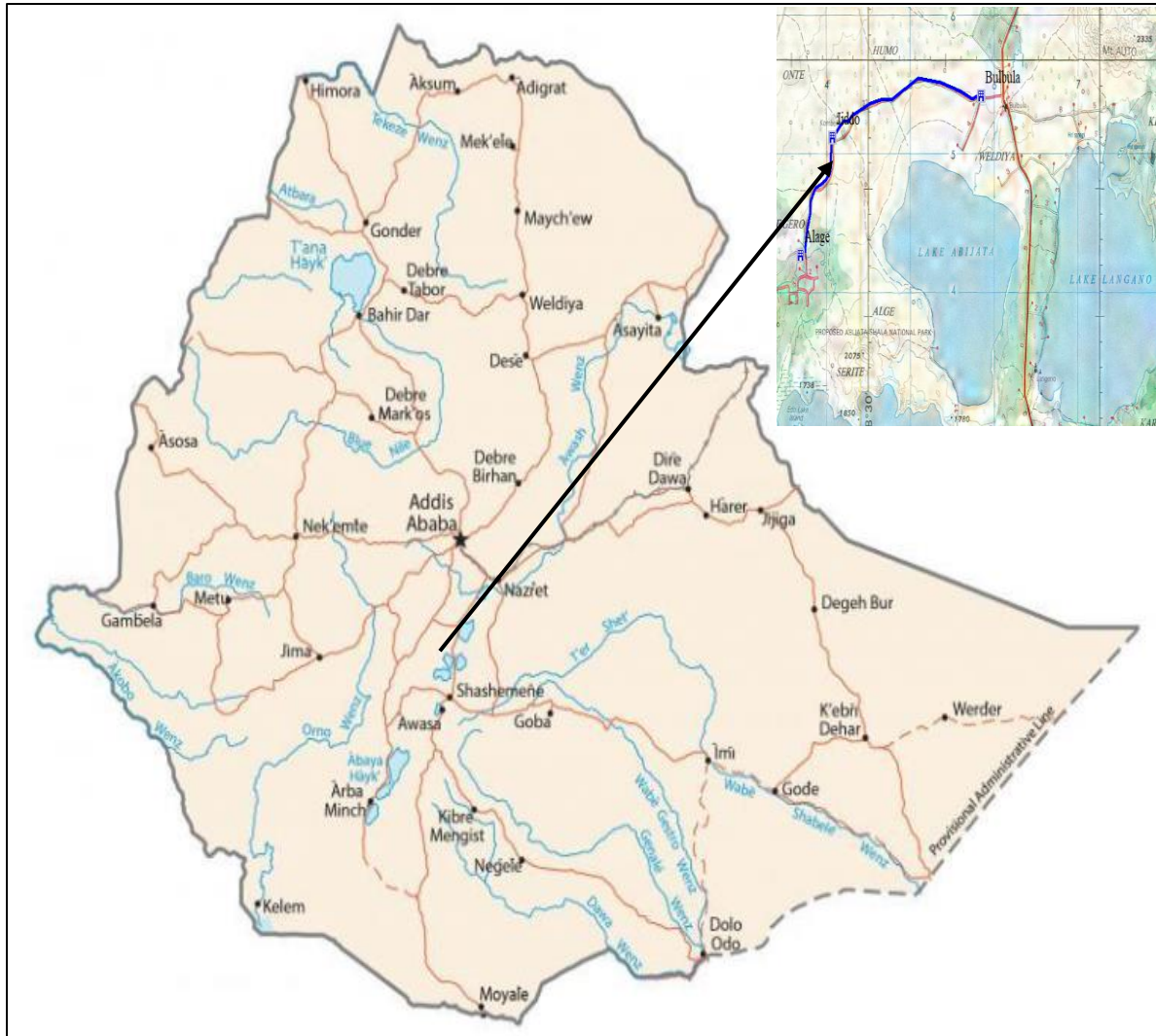


Figure 3-1: Location of the Pilot Route Corridor

### 3.2.2 Climate

Climate is influenced by latitude, altitude, land and water surfaces, mountain barriers, local topography, and such atmospheric features as prevailing winds, air masses and pressure centers.

The highest day time temperature recorded around Bulbula – Alage project route area is during the month of March and lowest daytime temperature is recorded during the month of November. The mean monthly maximum temperature at Alage station is 39.5 degrees Centigrade (°C). The mean monthly minimum temperature at Alage station is 0 degrees Centigrade (°C). The mean annual temperature is 20°C. Detail climatic data around Alage is shown in Table 3-2.

## Use of DCP and CBR tests to Characterize Subgrade Shear Strength

Project route area falls within semi-arid climactic zone. The mean maximum Rainfall at Alage area is from July to August. The mean annual rainfall is 708 mm.

**Table 3-2: Basic Climatic Data of the Project Area (Alage Area)**

Months of the Year	Rainfall (mm)		Temperature (°C)		
	Mean	80% Dependable	Max.	Min.	Mean
January	13.1	12.8	33.0	4.5	18.40
February	29.1	27.7	34.5	5.5	20.75
March	58.0	52.6	39.5	6.0	21.55
April	73.0	64.5	35.0	8.5	22.20
May	75.5	66.4	36.0	7.0	21.30
June	69.9	62.1	33.0	8.0	20.50
July	140.2	108.8	33.5	11.0	20.05
August	113.9	93.1	31.5	11.0	19.85
September	82.0	71.2	35.0	10.5	20.10
October	36.4	34.3	35.5	5.5	19.80
November	11.8	11.6	35.5	0.0	19.10
December	5.1	5.1	32.0	4.5	18.10
Mean Annual	708.0	610.2	34.5	6.83	20.10

### 3.2.3 Geological Setting

The Bulbula – Alage area is covered by different types of rock and soil formations emanating from weathering of different types of parent rocks and alluvial/lacustrine deposited materials. The route corridor is covered by quaternary geologic timescale period material formations and subgrade soil emanating from alluvial/lacustrine deposited material and/or weathering of parent material, (Mohr, P.A., 1966). As per the Geological map of Ethiopia, 1996 edition, geological formation available along the Bulbula – Alage project route is shown in Figure 3-2 and summary of the geological formation is included in Table 3-3.

Table 3-3: Geological Formation

Symbol	Geological Description	From	To
Q	Alluvial and Lacustrine deposits (Q): sand, silt, clay, diatomite, limestone and beach sand	0+000	29+093

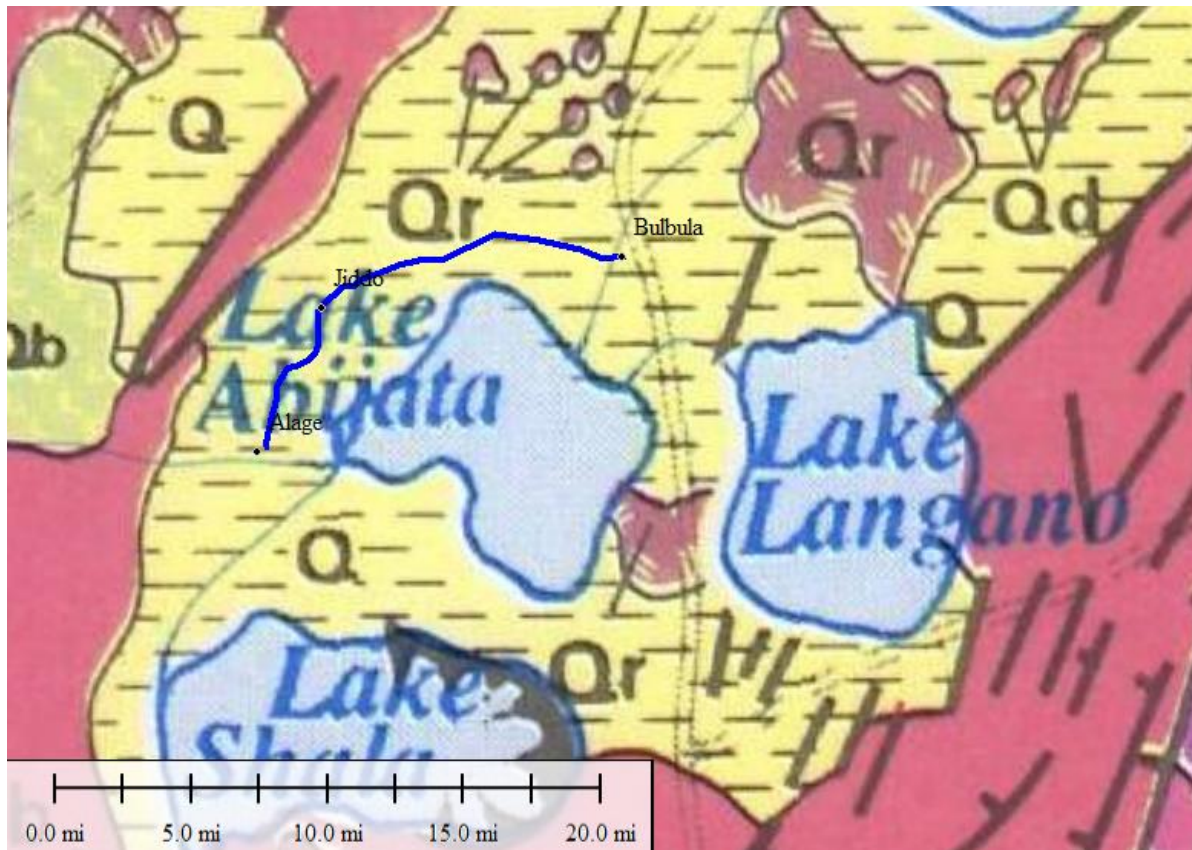


Figure 3-2: Geological Formation (Mengesha, T., et al, 1996)

### 3.2.3.1 Quaternary Formations (Q)

Quaternary Sediments of different origin (lacustrine, Aeolian, alluvial, marine) are widely spread all over Ethiopia. In the Main Ethiopian Rift, the Quaternary Sediments are mostly of lacustrine origin. Lacustrine beds are interbedded with Plio-Pleistocene pyroclastic in the lake region and, on the rift shoulders, (Mohr, P.A., 1966). The lacustrine beds are mostly redeposited volcanic sands, tuff with calcareous material and diatomite. At the beginning of the Quaternary an ancestral lake which was almost certainly continuous from the Abaya – Chamo Lakes to the south to the Awash basin to the north existed until it shrinks to smaller ones by late Pleistocene tectonic movements, (Mohr, P.A., 1966).

### 3.3 Field Investigation

Detailed site survey and investigation works were conducted to assess overall conditions of the pilot stretch area and to collect all the relevant information required for the research work. The field investigation along the project route includes broadly:

- Reconnaissance soil survey along the entire road section,
- Collecting soil sample for the laboratory testing,
- Undertaking field tests on soil.

#### 3.3.1 Subgrade Soil Investigations

The soil investigation was aimed at assessing actual condition of the alignment material which includes reconnaissance soil survey, DCP testing, density testing, sampling and logging of center line material for laboratory testing. The purposes of the soil investigation work are:

- To assess depth and nature of centerline materials along the route corridor,
- To assess in situ strength of the subgrade material,
- To characterize properties of centerline materials.

#### 3.3.2 Reconnaissance Soil Survey

In order to see the lateral extent of the alignment soil, soil survey was conducted along the entire road section. The soil survey along the road corridor is carried out by visual observation of color, texture, moisture and appearance of the soil along the road side and from test pits dug.

Soil with nearly similar type were grouped together and their extent was determined. As seen from visual soil survey, pyroclastic deposit has predominately covered significant section of the route. As seen and confirmed from the excavated boreholes, thickness of the deposit exceeds 5 m in majority of the stretches. Some of the various types of in-situ soil that exist along the route corridor are shown in Table 3-4 and the pyroclastic deposit is shown in Figure 3-3.

**Table 3-4: Soil Extension Survey**

Station		Description
From	To	
0+000	8+100	Pyroclastic deposit
8+100	8+300	Upper 50cm brown alluvial sand deposit, from 50 cm to 150 cm light creamy pyroclastic deposit
8+300	10+000	Pyroclastic deposit
10+000	11+400	Upper 50cm organic brown Pyroclastic deposit, from 50 cm to 150 cm light creamy Pyroclastic deposit
11+400	14+800	Upper 30cm brown SILTY sand, from 30 cm to 150 cm light creamy Pyroclastic deposit
14+800	14+900	Light grey pyroclastic deposit
14+900	16+100	Pyroclastic deposit
16+100	16+700	Highly Welded tuff
16+700	16+900	Welded tuff
16+900	17+100	Pyroclastic deposit
17+100	18+700	Upper 30cm brown silty sand, from 30 cm to 150 cm light creamy pyroclastic deposit
18+700	19+600	Brown SILTY sand
19+600	23+700	Pyroclastic deposit
23+700	24+600	Brown SILTY sand
24+600	27+800	Pyroclastic deposit
27+800	29+100	Upper 50cm brown SILTY sand, from 50 cm to 150 cm below light creamy pyroclastic deposit



**Figure 3-3: Pyroclastic Deposit**

### **3.3.3 Subgrade Material Sampling and Testing**

#### ***3.3.3.1 Index and Strength Tests***

To determine engineering properties of the soil along the road alignment, representative disturbed samples were collected by digging test pits along the design centerline. A test pit of approximately - 1.0 m x 1.0 m wide are excavated up to 1.5 m depth below the existing ground level. Within the 29 km total length of road fifty-seven samples have been tested with classification tests (sieve analysis and Atterberg limit) and twenty-nine samples have been tested with proctor and CBR tests. The average testing interval was 500 m for classification and 1 km for all test. The testing was undertaken in the site laboratory.

For the sole purpose of this research, additional ten test pits were excavated and samples collected from the upper and lower layers of the test pits. In order to have identical samples for CBR and direct shear testing, a single sample retrieved from site was quartered. The quartered sample was used for CBR and direct shear testing purpose. Eighteen samples were retrieved from site for this research purpose and tested with CBR and direct shear tests. The average additional sampling interval for direct shear and CBR testing was 3 km. The CBR test was undertaken in Beza consulting engineers Plc central laboratory and the direct shear test was tested in Lidet consulting engineers Plc central laboratory.

The lithological soil formations were properly logged. Bulk sample of about 60 kg was taken for laboratory testing. Finally, after completing the logging and sampling, the test pits

were backfilled, compacted and leveled off to their original level. Samples of excavated test pits are shown in Figure 3-4.



**Figure 3-4: Excavated Test Pits**

### ***3.3.3.2 Dispersive Soil Characterization Tests***

Dispersive clays have a higher relative amount of dissolved sodium in the pore water than regular erosion-resistant clays. When soils are sodic, which means they contain enough sodium to affect the structural integrity of the soil. Clay particles contain a negative surface charge that is balanced by positively charged cations like  $\text{Ca}^{2+}$ ,  $\text{Mg}^{2+}$ ,  $\text{K}^{+}$ , and  $\text{Na}^{+}$  that are dispersed throughout the clay's surface. The total number of exchange sites (the total capacity of a soil to hold exchangeable cations) in a particular amount of soil is measured by the cation exchange capacity (CEC). Clay particles are less closely linked to one another when the sodium to other ion ratio at these exchange sites is high, as a result the soil aggregates easily disperse when the soil is wet, (ERA, 2013).

Identification of dispersive soils started with field reconnaissance investigations to determine if there are any surface indications such as unusual erosion patterns with tunnels and deep gullies, concurrent with excessive turbidity in any storage water. Laboratory tests have been developed for identification of dispersive soils because the common laboratory index tests, such as visual classification, grain size analysis, specific gravity, or Atterberg limits, cannot distinguish dispersive clays. In order to check dispersion potential of the subgrade soil the following mineralogical tests have been undertaken on the subgrade sample retrieved from site within 5 km interval, the testing was undertaken in Ethiopian Construction Design and Supervision Works Corporation (ECDSWC) central laboratory.

- The exchangeable sodium percentage (ESP) and cation exchange capacity (CEC),
- Double Hydrometer Test Method (ASTM D-4221),
- Crumb test (ASTM D-6572),

### *3.3.3.3 Collapsible Soil Characterization Test*

Any unsaturated soil that undergoes a significant particle rearrangement and significantly reduces in volume upon wetness, further loading, or both is referred to as a collapsible soil. Typically, these soils have a loose soil structure, i.e., a large void ratio and water content far less than saturation. The finer silt and/or clay percentage, or possibly surface tension in the water at the air-water interfaces, operate as adhesives at the contact points of the coarser particles that make up the structure of these low-unit weight, unconsolidated sediments, (Woldechirkos, Y., and Desaleg, K., 2020).

Collapsible soils show relatively high apparent strength in their dry state, but have low density, porous structure and are susceptible to large deformations upon wetting due to sudden large reduction in their volume.

The addition of water is a widely used explanation for triggering soil collapse. Collapse can also occur, however, as the result of load application, or wetting, or both. In any condition of the physical basis of the bond strength, all collapsible soils are weakened by the addition of water. Decreased strength is more immediate in cases where the grains are held together by capillary suction, slow in the case of chemical cementing, and much slower in the case of clay buttresses (clay between the sand particles which provides additional support).

The addition of water to a collapsible soil causes the bonding or cementing agent to be reduced and the inter-granular contents to fail in shear resulting in reduction in total volume of the soil mass. The settlement of a collapsing soil is more or less immediate and occurs upon the intake of moisture by the soil. The severity of collapse depends on the extent of wetting, depth of the deposit and loading from the overburden weight and structure, in any case where collapse is suspected water shouldn't pond near the road infrastructure.

The amount of collapse normally depends on the initial void ratio, stress history of the soil, thickness of the collapsible soil layer and magnitude of the applied stress. To estimate the magnitude of potential collapse in an area, a one-dimensional collapse potential test (ASTM D-5333) is undertaken on the subgrade sample retrieved from site within 5 km interval in (ECDSWC) central laboratory.

### 3.3.4 Dynamic Cone Penetrometer Test (DCP Testing)

Dynamic Cone Penetrometer test (DCP test) was carried out for the determinations of in-situ strength of the pyroclastic deposit. In a single test pit of approximately 1.5 m depth, two DCP tests were undertaken. The DCP test was undertaken adjacent to the point where field density test was conducted. The average testing interval was approximately 3 km.

If there is no penetration under 20 consecutive blows and the hammer is bouncing upon falling on the coupling drive seat, the test point was shifted and another trial was carried out before the test was terminated.

The DCP test was extended up to a depth of 1000 mm below the subgrade. However, for some sections of the road, the hard surface totally obstructs penetration of the cone and termination of the test before 1 m penetration is attained. The DCP test was undertaken approximately 20 cm from the existing ground level and at the bottom of the test pit at a depth of about 1.5 m below the existing ground level as shown in Figure 3-5.

The DCP test was conducted using 8 kg hammer freely falling from a height of 575 mm driving a 60° cone having a base diameter of 20 mm. While the cone penetrates through the layer, depth of penetration with corresponding number of blows was read in mm from a fixed meter ruler. The DCP test result in some sections of the route corridor confirmed that the subgrade material is firm and intact.



**Figure 3-5: DCP Test**

### 3.3.5 In-Situ Density Test

Field density test was conducted by using sand replacement method. The test involves excavating a hole in the ground, filling the hole with calibrated sand using the sand cone apparatus, and then determining the volume of the hole based on the amount of sand required to fill the hole.

Before commencing the test, the surface was trimmed and smoothed to form a suitable seat for the measuring apparatus. Then, a hole was dug through guide of the base plate. The material from the test hole was carefully collected as specified in AASHTO T-191 into a polythene bag whereby it has been weighed, tightly sealed and labeled for natural moisture content determination. Sand with known unit weight was then poured into the hole through a sand cone from a sand jar with measured weight.

After determining wet mass of the soil, it was divided by the volume of the hole to obtain the wet density (bulk density) of the material. In-situ moisture content was determined during density testing. The dry density is then determined from the natural moisture content and wet density using the following relation,

$$\gamma_d = \frac{\gamma_{wet}}{1 + \omega} \quad 3.1$$

Where  $\gamma_d$ = dry density,  $\gamma_{wet}$ = wet density,  $\omega$ = natural moisture content

Finally, the level/degree of compaction is computed as the ratio of the field dry density to the laboratory maximum dry density.

$$\text{Level Compaction} = \frac{\gamma_d}{MDD} * 100 \quad 3.2$$

In-situ density test was conducted within an average interval of 3 km inside of the test pits as shown in Figure 3-6.



**Figure 3-6: Field Density by Sand Replacement Method (on the Upper and Lower Layer)**

## CHAPTER 4 ANALYSIS OF FIELD AND LABORATORY TEST RESULTS

### 4.1 Introduction

Field and laboratory tests undertaken have been analyzed in order to assess and determine the behavior of existing subgrade material. The sampled soils were tested in different laboratories. In addition to tests undertaken for this research purpose, the test results executed for the design and construction of Bulbula - Alage road project have been used in order to characterize the soil. In performing the laboratory tests, AASHTO, ASTM and BS standard testing methods have been adopted.

### 4.2 Laboratory Test Results

#### 4.2.1 Atterberg Limit

An indication as to the nature of the soil may be given by the variation in Plasticity Index (PI). The PI is influenced by the type and proportion of clay minerals present; high PI values are often indication of the potential expansive nature of the soil. The variation of PI along Bulbula – Alage route corridor is presented in Figure 4-1. The results revealed that plasticity values of the subgrade materials along the stretch is dominantly low to none (i.e., material having plastic index of  $< 20\%$  and liquid limit of  $< 50\%$ ).

The plasticity chart of Figure 4-2 helps to classify the type of soils based on their plasticity characteristics (i.e., Atterberg Limits and Indices of soils). Generally, materials falling above the A-Line are classified as clays and below the A-Line are classified as silts. The line labelled “A” above a liquid limit of 50 separates soils of high plasticity, or fat clays (above line), from elastic clay/silt, soils of low compressibility (below line). At liquid limits less than 50, line “A” separates soils of medium plasticity (above line) from soils of medium compressibility (below “A” line). Using this graph, critical lower limits for liquid limit and plasticity index can be ascertained. Soils that have high or very high shrinkage and swell potential would have liquid limits greater than 50 and plasticity indices greater than 30. Soils with moderate shrink-swell potential have liquid limits ranging from 35 to 50 and plasticity indices between 20 and 30. Low shrink-swell potentials are indicated by liquid limits less than 35 and plasticity indices less than 20.

As shown in Figure 4-2, majority of the subgrade soil along Bulbula – Alage route corridor belongs to the CL (inorganic clay of low to medium plasticity) and ML (inorganic silts of low plasticity) family of Indian and/or unified soil classification system (UCS).

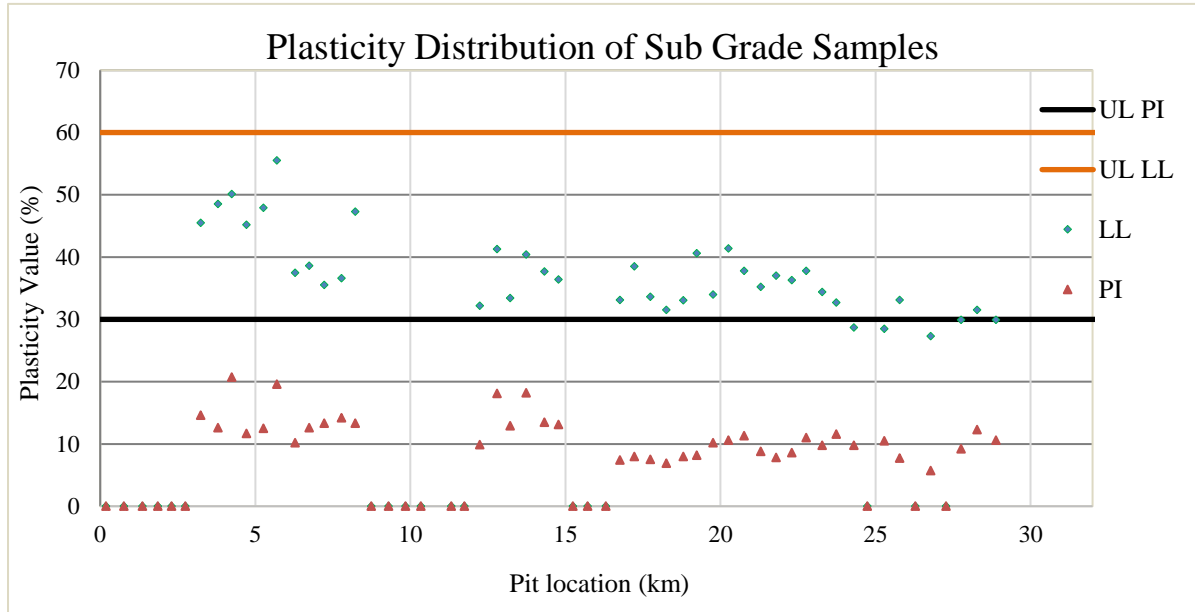


Figure 4-1: Variation of Plasticity Index (%) of the Subgrade soils

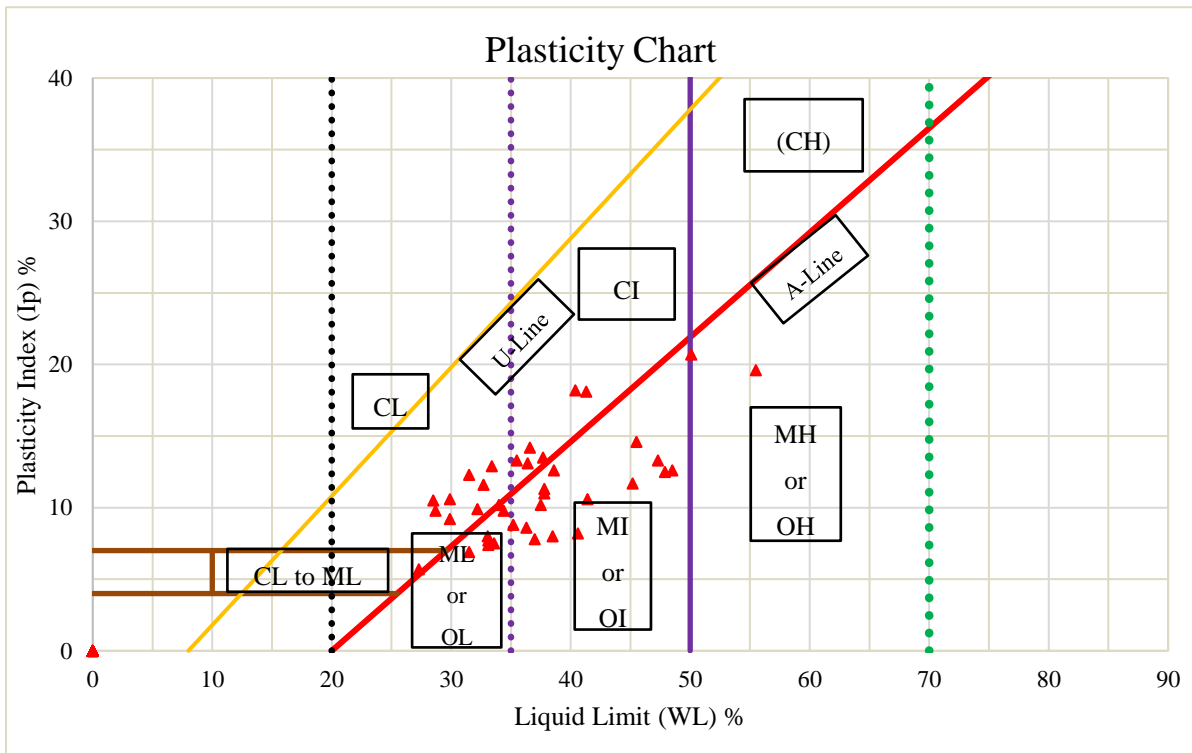


Figure 4-2: Plasticity Chart of the Subgrade Soil (ISC/UCS)

### 4.2.2 Particle Size Analysis

Particle size distribution represents the distribution of particles of different sizes in the soil mass. The behavior of coarse-grained soils is extremely dependent on the particle size distribution and behavior of fine-grained soils (minus 75  $\mu\text{m}$ ) depends upon plasticity characteristics. The Plasticity behavior of a soil is influenced by the type and proportion of clay particles present within the material.

Particle Size Distribution tests have been carried out on samples recovered from the trial pits. The results are summarized in Figure 4-3 in terms of the percentage of silt and clay (< 0.075 mm), the percentage of fine and medium sand (0.075 mm - 0.425 mm), percentage of coarse sand (2 mm - 0.425 mm) and gravel (2 mm – 75 mm).

From the particle size distribution curve, the soil along the route corridor from station 3+240 to 8+740 and 17+220 to 21+300 (32 % from the total stretch) is majorly dominated by silt and clay fractions (i.e., in the specified stretch more than 52 % fraction is silt/clay and 48 % is sand & coarse particle fraction). Thus, it can be concluded that, station 3+240 to 8+740 and 17+220 to 21+300 soil mass is majorly classified as fine grained in both AASHTO and USC soil classification systems. The soil along the project route corridor from station 0+000 to 3+240, 8+740 to 17+220 and 21+300 to 29+100 (68 % from the total stretch) is majorly dominated by fine and medium sand and coarse particles fractions (i.e., in the specified stretch more than 52 % fraction is sand & coarse particle and 48 % fraction is silt/clay). Thus, it can be concluded that, station 0+000 to 3+240, 8+740 to 17+220 and 21+300 to 29+100 section soil mass is majorly classified as coarse grained in the USC soil classification system.

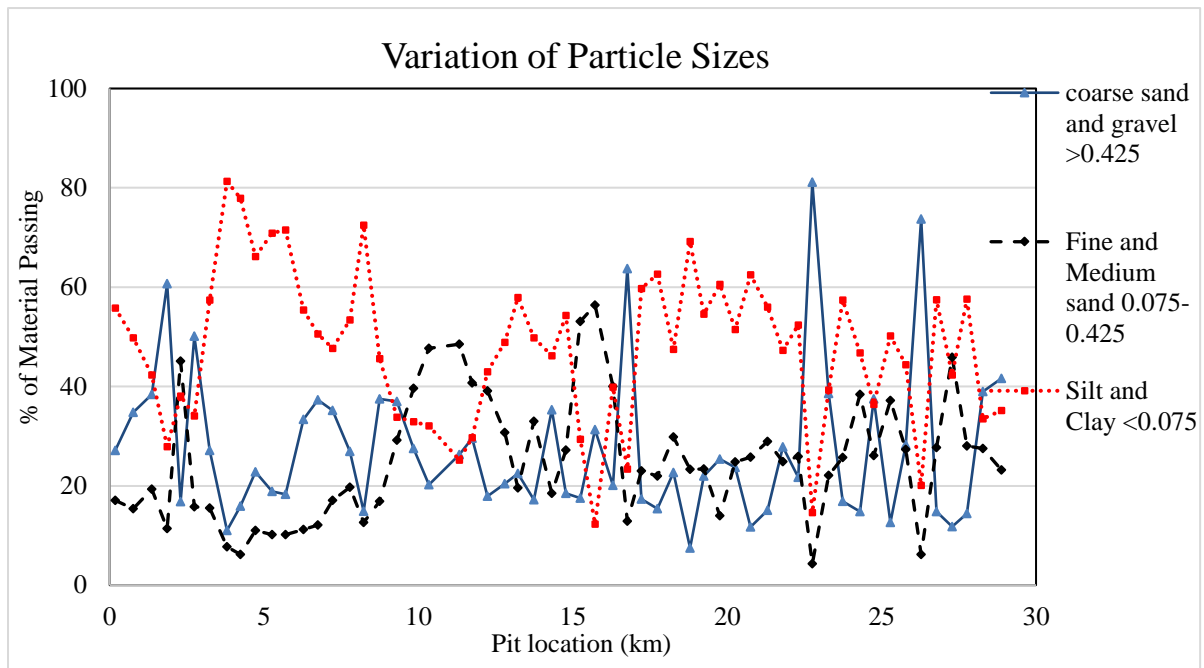


Figure 4-3: Particle Size Distribution of Subgrade Soils along the Road Alignment

#### 4.2.3 Soil Classification

The engineering classification of soils is the most universally accepted indicator of the physical property of a naturally occurring soil. The AASHTO and UCS methods of soil classification are the methods most commonly accepted in construction sector. This procedure relies on the grain size distribution and plasticity characteristics of the soil to differentiate between soils.

According to AASHTO soil classification system, the soil along the alignment falls into A-4, A-2-4, A-6, A-7-5, A-7-6, A-2-6, A-1b and A-5 soil groups. However, the majority of the soil along the alignment belongs (more than 75%) to A-4, A-2-4 and A-6 AASHTO soil groups.

As per USC classification system, the soil belongs to SM (silty sand), MI (inorganic silts of medium plasticity), SC (clayey sand), ML (inorganic silts of low plasticity), CI (inorganic clay of medium plasticity), CL (inorganic clay of low plasticity), MH (inorganic silts of high plasticity), SP to SC and CL to ML groups. The majority of the route corridor subgrade material (more than 89%) belongs to SM, MI, SC and ML groups.

Taking the index tests into consideration (Atterberg limit and gradation), the subgrade material of the route corridor is low plasticity silty/clayey sand. The percentage composition is shown in Figure 4-4.

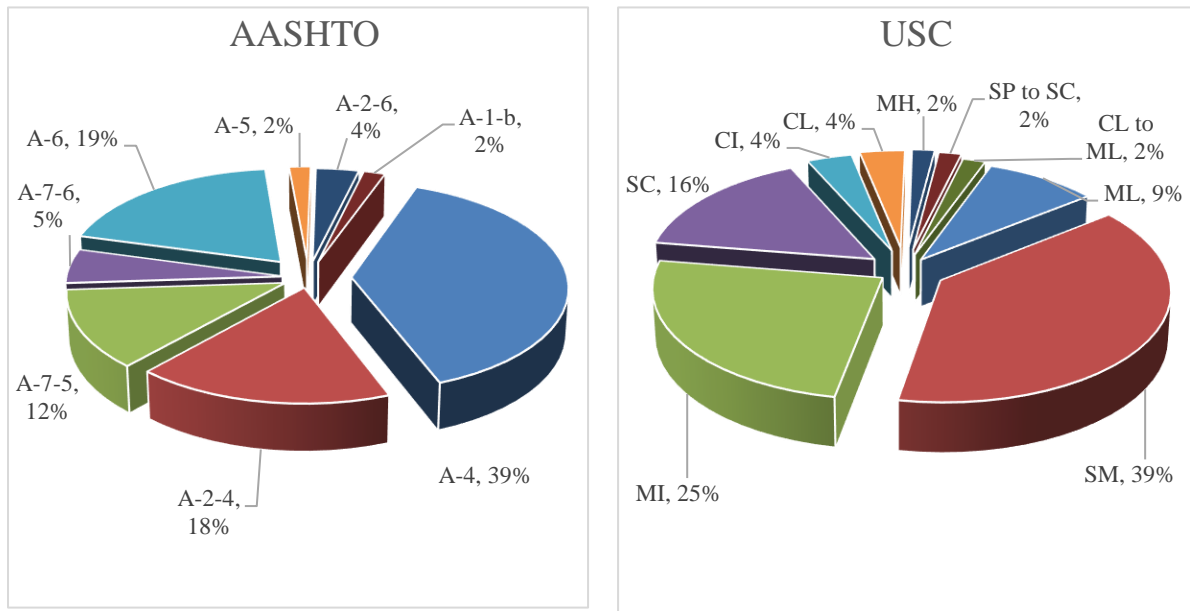


Figure 4-4: Percentage Compositions of Soil Classification

#### 4.2.4 Evaluation of Collapsibility of the Soil

The laboratory tests undertaken to analyze collapsibility of subgrade material of the route corridor is undertaken in Ethiopian Construction Design and Supervision Works Corporation.

The test method consists of placing a soil specimen at natural water content in a consolidometer, applying a predetermined applied vertical stress to the specimen and inundating the specimen with fluid to induce the potential collapse in the soil specimen. A collapsible soil may withstand relatively large applied vertical stress with small settlement while at a low water content, but this soil will exhibit settlement (that could be large) after wetting with no additional increase in stress. The one-dimensional collapse potential test result obtained on the soil sample retrieved from site is shown in Table 4-1.

$$I_c(\text{Collapse Potential, \%}) = \frac{\Delta h}{h_0} * 100 \quad 4.1$$

Where:

$\Delta h$  = change in specimen height resulting from wetting, mm

$h_0$  = Initial specimen height, mm

**Table 4-1: Collapse Potential Test Result**

Laboratory	Station						
ECDSWC Laboratory Test	0+000	5+000	10+000	15+000	20+000	25+000	29+151
Result (%)	7.48	5.7	7.24	10.52	8.09	6.94	7.00
Remark: – collapse potential 0 – 1 % indicates there is no severity of problem collapse potential 2 – 5 % indicates there is slight severity of problem collapse potential 6 – 10 % indicates there is moderate severity of problem collapse potential 11 – 20 % indicates there is severe severity of problem collapse potential > 20 % indicates there is very severe severity of problem							

As we can see from Table 4-1, the one-dimensional collapse potential test result of the subgrade varies between 5.7 – 10.5 %. Based on the test result it is moderately collapsible material.

#### **4.2.5 Evaluation of Dispersiveness of the Subgrade**

To check the extent or rate of dispersiveness of Bulbula – Alage route corridor soil, the samples were tested with chemical test, double hydrometer test and crumb test. These tests are recommended by ERA manual as an identification for dispersive soil.

##### **4.2.5.1 Chemical Test Analyses**

Chemical tests undertaken on the soil samples helped us to know the chemical composition and proportion of the clay minerals, especially the cation exchange capacity and/or exchangeable sodium ion of the clay and the extent to which the clay is expected to be dispersive by analyzing the chemical composition. The result obtained is shown in Table 4-2.

**Table 4-2: Chemical Test Result**

Station	Test Result (cmol (+)/kg or meq/100g)						
	Na <sup>+</sup>	K <sup>+</sup>	Ca <sup>++</sup>	Mg <sup>++</sup>	Sum	CEC	ESP (%)
0+000 LHS	2.81	6.12	20.65	4.13	33.71	34.12	8
5+000 CL	2.1	6.93	7.26	2.82	19.11	19.72	10
10+000 LHS	2.05	6.21	14.3	4.09	26.64	26.65	8
15+000 RHS	1.22	0.94	22.02	5.51	19.7	39.59	3

## Use of DCP and CBR tests to Characterize Subgrade Shear Strength

20+000 RHS	1.27	5.43	21.16	5.08	32.94	44.63	3
25+000 LHS	1.37	2.32	31.9	7.23	42.82	42.99	3

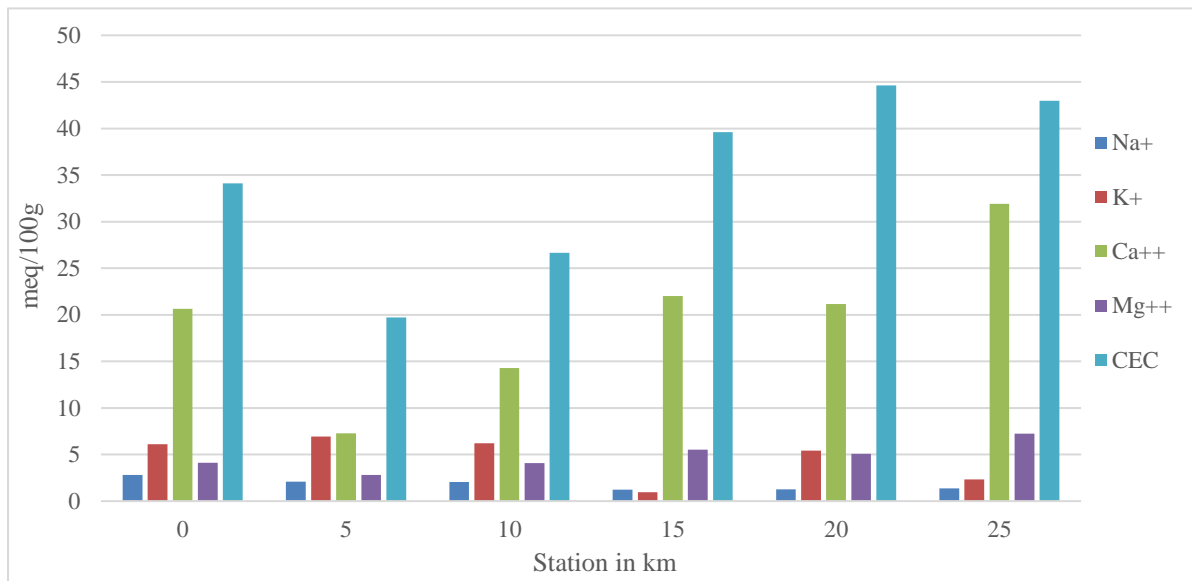


**Figure 4-5: Cations Composition in the Soil**

As seen from the test result, cation exchange capacity of the subgrade soil varies from 19 meq/100gm to 44 meq/100gm. CEC is expressed in terms of either mill equivalents of adsorbed cations per one-hundred grams soil (meq/100g), or centimoles of charge per kilogram (cmol(+)/kg).

The section from station 15+000 to 29+000 have higher CEC value than the section from 0+000 to 15+000. When we compare the individual cations, the sodium and potassium ion concentration in the soil from station 0+000 to 15+000 is higher than that of station 15+000 to 29+000. The calcium and magnesium ion concentration in the soil from station 0+000 to 15+000 is lower than that of station 15+000 to 29+000. Calcium and magnesium stabilize soil structure, the calcium that is adsorbed to soil particles helps in stabilizing the soil structure. Adsorbed sodium causes the soil to disperse when wet. Calcium replaces the adsorbed sodium and result in stable soil structure. The cations and CEC values obtained from laboratory testing is shown in Figure 4-5.

The presence of excessive amounts of exchangeable sodium reverses the process of aggregation and causes soil aggregates to disperse into their constituent individual soil particles. Deflocculation occurs because unlike the polyvalent cations of calcium and aluminum, sodium is monovalent.

A sodic/dispersive soil contains a high level of sodium relative to the other exchangeable cations (i.e., calcium, magnesium and potassium). As per ERA site investigation manual 2013 soils are classified into 4 dispersion classes (non-sodic, < 6%, slightly sodic, 6 – 10 %, Moderately sodic, 10 – 15 %, highly sodic, > 15 %,) based on the percentage of sodium ion relative to others. Based on the test result: - station 0+000, 5+000 and 10+000 subgrade soil are slightly sodic and station 15+000, 20+000 and 25+000 subgrade soil are non-sodic.

***4.2.5.2 Double Hydrometer Test Analyses***

The soil conservation service (SCS) double hydrometer test is one of the primitive methods developed to assess the dispersiveness of soils. The test assesses the dispersity of soil by comparing the natural tendency of the clay fraction in the soil to go into suspension in water with an identical test in which conventional dispersants and mechanical breakdown are used. The procedure involves determination of the percentage of particles in the soil that are finer than 0.005 mm using the standard hydrometer test for particle size distribution. A parallel test is carried out, in which no chemical dispersant is added and the sample is not mechanically agitated. The quantity of particles finer than 0.005 mm in the parallel test is expressed as a percentage of this fraction determined in the standard test, which is defined as the dispersion ratio or dispersity of the soil (Elges, 1985). Soils having dispersion ratios greater than 50 % are considered highly dispersive, between 30 and 50 % are moderately dispersive and below 30 % are non-dispersive (Elges, 1985). Summary of the double hydrometer test result is shown in Table 4-3.

**Table 4-3: Double Hydrometer Test Result**

Laboratory	Station						
	0+000	5+000	10+000	15+000	20+000	25+000	29+151
ECDSWC laboratory test result (%)	31.65	36.26	34.99	34.10	43.99	33.99	35.75

The test results of double hydrometer and exchangeable sodium ion percentage shows, the subgrade soil of the route corridor belongs to non-dispersive to moderately dispersive class.

**4.2.6 Moisture – Density Relationship**

A proctor compaction curve (AASHTO T99 or T180) indicates maximum dry density and optimum moisture content which are the two principal output values from this test. It must be remembered that each soil has a unique relationship of moisture content and maximum

dry density that must be established in the laboratory. It is critical to select a moisture density specification that ensures a specific level of physical performance in the soil. The moisture density state of a compacted soil affects strength and deformation characteristics of soil in the pavement which is related to its structural adequacy.

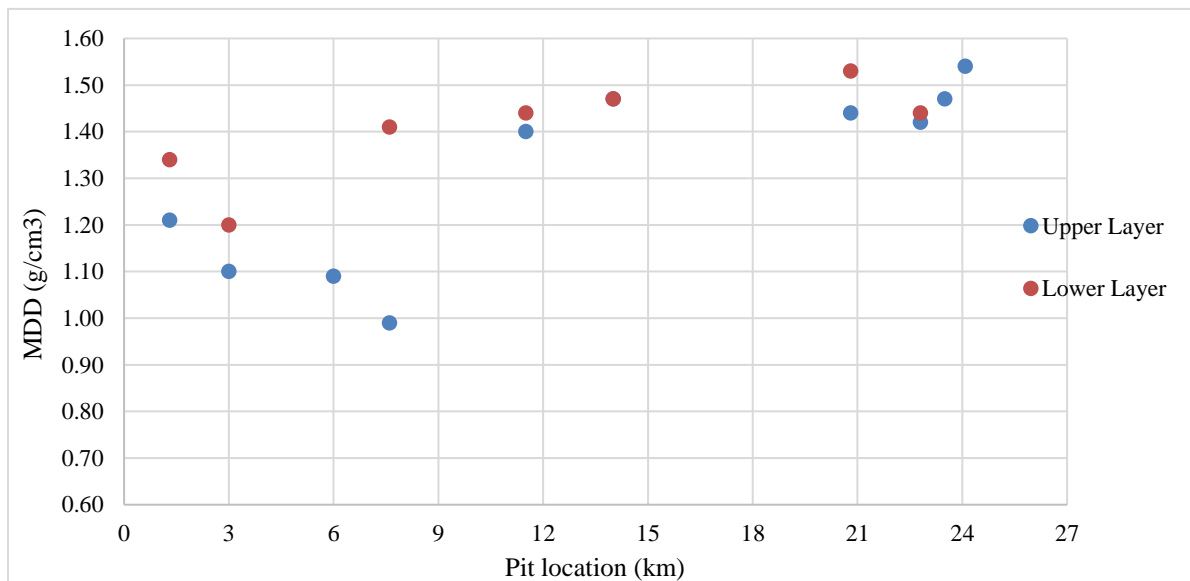
Soil samples obtained from test pits have been compacted in the laboratory at various moisture contents to derive dry density versus moisture content relationships. Compaction tests were carried out according to AASHTO T-180 on samples recovered from the test pits. The maximum dry density (MDD) and optimum moisture content (OMC) values obtained from the laboratory tests are summarized in Table 4-4.

**Table 4-4: Maximum Dry Density and Optimum Moisture Content of the Subgrade**

Upper Layer										
Pit location (km)	<b>1.30</b>	<b>3</b>	<b>6</b>	<b>7.6</b>	<b>11.5</b>	<b>14</b>	<b>20.6</b>	<b>22.8</b>	<b>23.5</b>	<b>24.08</b>
Optimum moisture content %	26	20	28	37	20	22	23	24	25	22
Maximum dry density ( $g/cm^3$ )	1.21	1.10	1.09	0.99	1.40	1.47	1.44	1.42	1.47	1.54

Lower Layer								
Pit location (km)	<b>1.30</b>	<b>3</b>	<b>6</b>	<b>7.6</b>	<b>11.5</b>	<b>14</b>	<b>20.6</b>	<b>22.8</b>
Optimum moisture content %	21	22		19	24	21	22	24
Maximum dry density ( $g/cm^3$ )	1.34	1.20		1.41	1.44	1.47	1.53	1.44



**Figure 4-6: Maximum Dry Density of the Tested Pits**

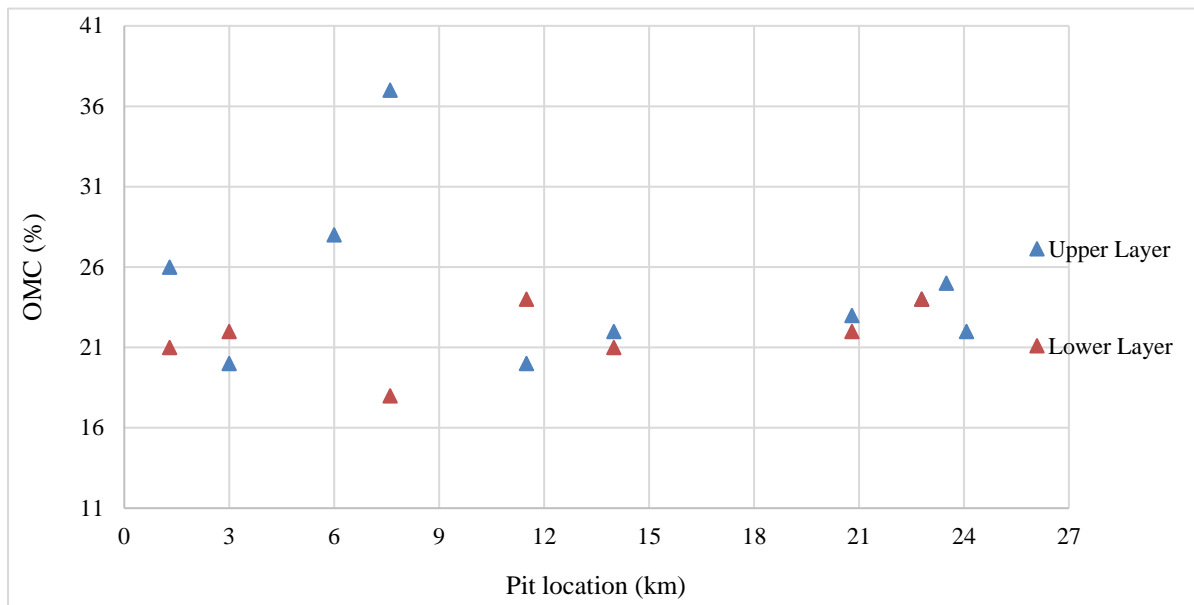


Figure 4-7: Optimum Moisture Content of the Tested Pits

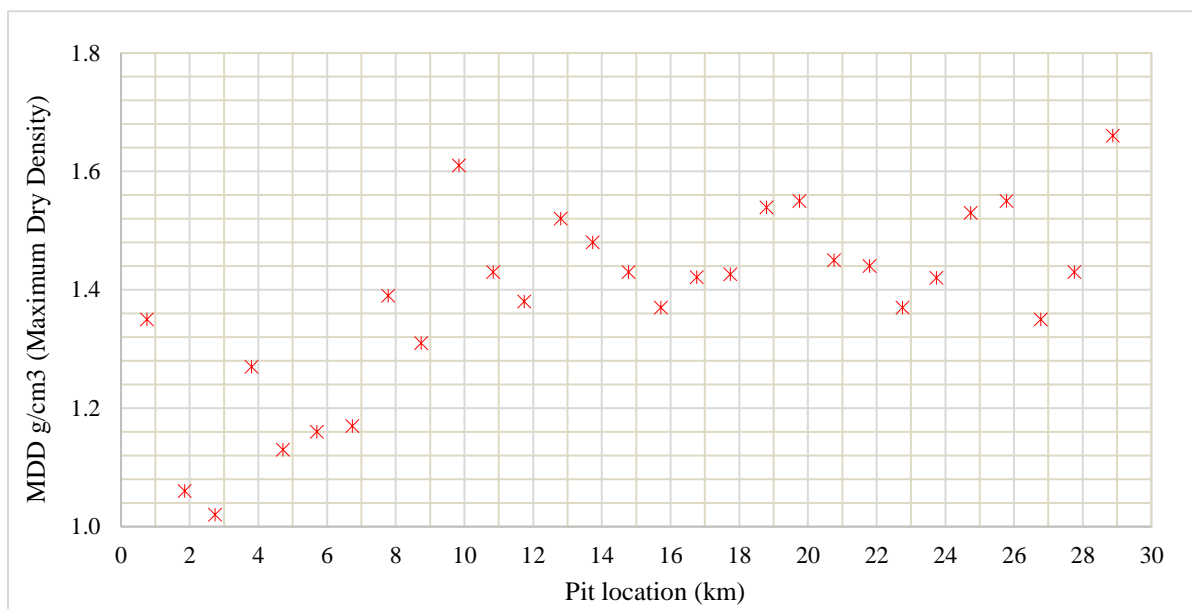


Figure 4-8: Maximum Dry Density (Proctor Test Undertaken During Bulbula – Alage Road Construction)

As seen from Figure 4-6 and Figure 4-8, the MDD value of the pyroclastic deposit in the majority of the stretch is below  $1.5 \text{ g/cm}^3$ . The volcanic ash/pyroclastic deposit have relatively low MDD value. The volcanic ash/pyroclastic deposit is a natural lightweight material which is light enough and yet strong enough to be used as construction material when compacted. The lightness is due to the escaping of gas from the molten lava when erupted from deep beneath the earth's crust. When lava cools quickly, it doesn't have a chance to form the large crystals, the lava rapidly cools into a lightweight material full of

holes, or pores. Those holes, full of air, are what keep the ash deposit afloat or have low density value.

Figure 4-7 shows that the optimum moisture content value is high. Due to porosity of the ash, the OMC value is expected to be higher. High vascularity in the volcanic ash results in higher OMC value.

The MDD value of the soil up to station 11+000 is  $\leq 1.4 \text{ g/cm}^3$ . The MDD value of the subgrade material from station 11+000 to Alage / (29+000) is majorly between  $1.4 \text{ g/cm}^3 - 1.55 \text{ g/cm}^3$ . The section from station 14+000 to 29+000 was formerly part of the Abiyata Lake, even if there is no difference in material type as per visual observation, it is indicated in section 4.2.5.1 that the calcium and magnesium ion concentration in this section is higher than the section between station 0+000 to 14+000. When compared to the single charged cations of Sodium and Potassium, Calcium and Magnesium stabilize soil structure. Station 14+000 to 29+000 was formerly part of the Abiyata Lake that, the load from Lake water will provide additional densification to the pyroclastic deposit, this will also improve the density of the deposit.

### 4.2.7 California Bearing Ratio (CBR)

Three-point CBR test (i.e., 10, 30 and 65 blows of the hammer) was undertaken in accordance with AASHTO T-193. This form of testing is preferred as it can give information of the variation of strength that can be developed with increasing compactive effort. When the material is strong, the CBR reading will be high and the required pavement thickness will be reduced, this gives considerable cost saving. Conversely if CBR test indicates the material is weak, the CBR reading will be low that a suitable thicker road pavement shall be constructed to spread the wheel load over a greater area of the weak subgrade in order that the weak subgrade material is not deformed, causing the road pavement to fail. CBR-swell values are also determined on remolded samples of soil recovered from trial pits along the road corridor to evaluate potential to heave of the material.

Table 4-5, Figure 4-9 and Figure 4-11 show CBR value of the pyroclastic deposit is relatively high. It is indicated in section 4.2.6 that, MDD value of the subgrade material is low. In the majority of circumstances volcanic ash deposits have low MDD and high CBR value. The pyroclastic deposit has low CBR swell value.

Table 4-5: CBR and CBR Swell Values of the Subgrade

Upper Layer										
Pit location (km)	1.30	3	6	7.6	11.5	14	20.6	22.8	23.5	24.08
CBR (%)	9	34	17	14	17	40	34	25	9	37
CBR swell (%)	1.95	1.66	1.91	1.71	1.91	1.69	1.49	1.68	1.60	1.76

Lower Layer								
Pit location (km)	1.30	3	6	7.6	11.5	14	20.6	22.8
CBR (%)	34	36		39	24	41	44	39
CBR swell (%)	0.94	1.42		1.46	1.66	1.60	0.96	1.49

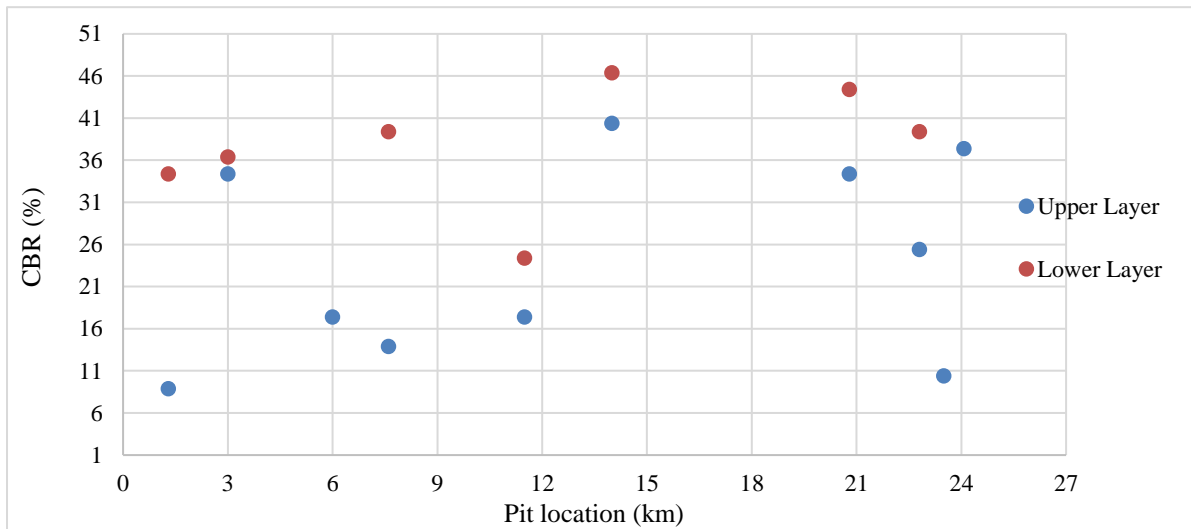


Figure 4-9: CBR Value of the Tested Pits

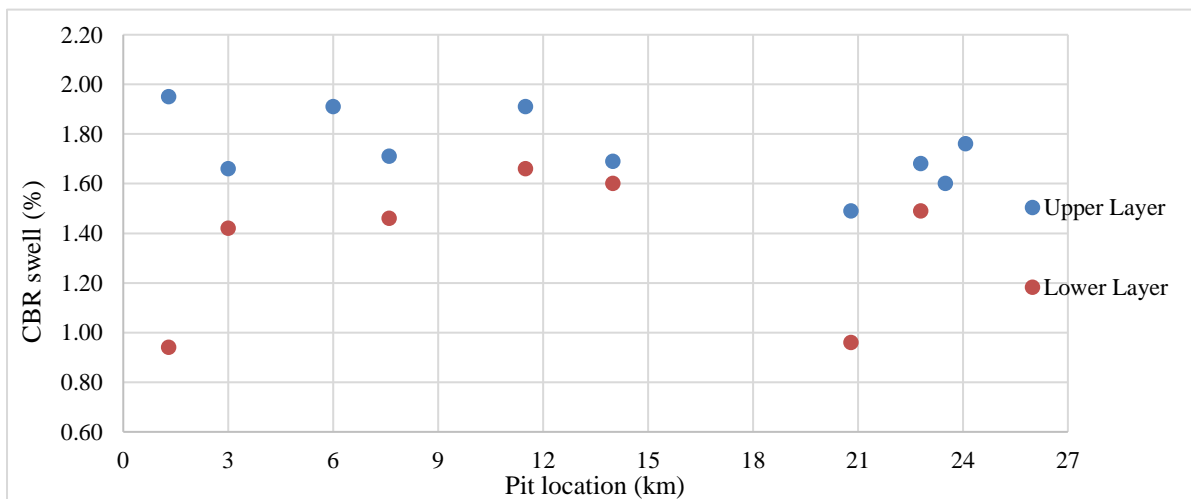
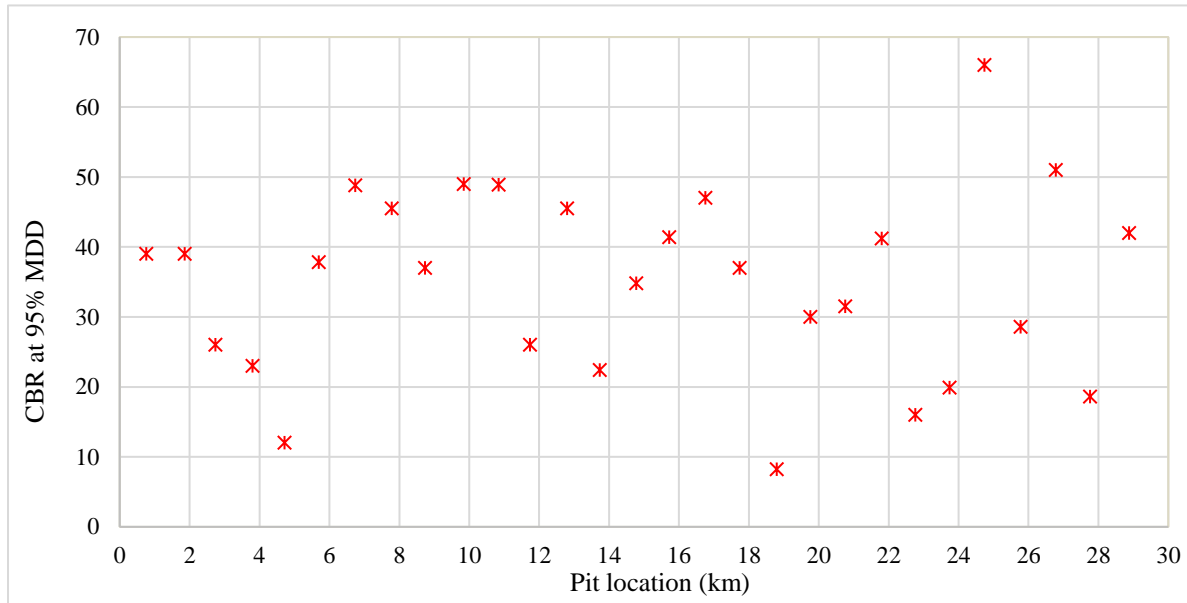


Figure 4-10: CBR Swell Value of the Tested Pits



**Figure 4-11: CBR Value (CBR Test Undertaken During Bulbula – Alage Road Construction)**

The CBR values obtained during the thesis work and road construction stage varies majorly between 15 % and 50 %. In both stages of testing, the CBR value obtained along the project route corridor is close to each other. Figure 4-9 indicates CBR value the pyroclastic deposit increase with depth. Subsurface layers are subject to the compacting weight of the soil above them. As depth increases, effective stress (unit weight \*depth) increases, this will result in densification and rearrangement of soil particles which results in higher strength.

Under normal scenario increase of strength and density of the material with depth is expected. The volume of air spaces between soil particles will decrease when depth increase due to compaction/densification effect from the upper layer. This increases the density, strength, and stiffness of the soil, making it more suitable for supporting heavy loads and resisting deformation.

### 4.2.8 Direct Shear Test

As per AASHTO T-236 and ASTM D-3080 consolidated drained shear strength of the pyroclastic deposit was measured by the direct shear test. During direct shear test, control on the drainage condition is very difficult and measurement of pore water pressure is not possible that it is difficult to guarantee beyond reasonable doubt whether the test is consolidated drained or not. But, as recommended in AASHTO T-236 and ASTM D-3080 by selecting proper normal force and time for consolidating the specimen and providing a low strain rate which consider the type of material to be tested, a near consolidated drained shear strength parameters can be obtained.

## Use of DCP and CBR tests to Characterize Subgrade Shear Strength

The test was performed by deforming a specimen at a controlled strain rate on a single shear plane determined by the configuration of the apparatus. The disturbed sample retrieved from site have been remolded to field dry density value for undertaking direct shear test. Three specimens from each sample have been tested at 100, 200 and 300-kPa vertical stress and subject to shear stress until failure. The cohesion and angle of internal frictions have then been computed.

As seen from Table 4-6, cohesion value of the pyroclastic deposit is extremely low to none. The material attains its strength from friction between intergranular particles. The average value of angle of internal friction is  $32.6^\circ$  and that of cohesion is 1.94 kPa. The distribution of grain size, angularity and particle interlocking are the main variables that affect a soils friction angle in addition to density. Fine grained and well-rounded sand has a lower friction angle than angular and coarse sand. In majority circumstances, angle of internal friction value between  $30^\circ - 40^\circ$  indicates medium dense soil and angle of internal friction value between  $20^\circ - 30^\circ$  indicates a loose soil. As per the direct shear test result, the subgrade soil in the majority section of the pilot route corridor is medium dense pyroclastic deposit.

**Table 4-6: Direct Shear Values of the Subgrade**

S/ No	Station (km)	Bulk density (g/cm <sup>3</sup> )	Dry density (g/cm <sup>3</sup> )	Moisture content (%)	Remolded Direct Shear (ASTM D-3080)	
					$\phi$ (°)	c (kN/m <sup>2</sup> )
1	1+300 Upper Layer	1.38	1.12	22.60	26.12	4.27
2	1+300 Lower Layer	1.62	1.35	19.90	41.02	1.00
3	3+000 Upper Layer	1.13	0.96	17.92	30.14	3.00
4	3+000 Lower Layer	1.34	1.11	20.61	31.74	0.11
5	6+000 Upper Layer	1.18	0.99	20.09	31.11	1.23
6	6+000 Lower Layer	1.22	1.01	21.00	33.01	1.40
7	7+600 Upper Layer	1.25	0.95	31.51	30.24	2.65
8	7+600 Lower Layer	1.27	1.08	17.58	31.14	0.22
9	11+500 Upper Layer	1.38	1.16	19.47	22.01	3.15
10	11+500 Lower Layer	1.61	1.34	20.50	33.96	0.54
11	14+000 Upper Layer	1.50	1.24	20.73	34.02	1.67
12	14+000 Lower Layer	1.73	1.43	21.10	39.17	0.25
13	20+600 Upper Layer	1.73	1.43	21.68	36.95	1.82
14	20+600 Lower Layer	1.70	1.42	20.09	34.86	1.80

## Use of DCP and CBR tests to Characterize Subgrade Shear Strength

15	22+800 Upper Layer	1.42	1.15	23.08	30.91	1.79
16	22+800 Lower Layer	1.42	1.40	22.50	38.89	1.09
17	23+500 Upper Layer	1.79	1.47	21.30	31.91	3.58
18	24+080 Upper Layer	1.34	1.11	19.81	29.02	5.42

### 4.3 Field Test Results

#### 4.3.1 Field Density Test

In-situ density test was conducted with sand replacement method as specified in AAHTO T-191. In each of the test pits two field density tests have been undertaken. On the upper section of the test pits; the test was undertaken approximately 25 cm below the existing ground level. Approximately 150 cm from the existing ground level another field density test was undertaken. The field density test result is shown in Table 4-7 and Figure 4-12.

**Table 4-7: Field Density by Sand Replacement Method**

<b>Upper Layer</b>										
Pit location (km)	<b>1.30</b>	<b>3</b>	<b>6</b>	<b>7.6</b>	<b>11.5</b>	<b>14</b>	<b>20.6</b>	<b>22.8</b>	<b>23.5</b>	<b>24.08</b>
Bulk density ( $g/cm^3$ )	1.24	1.09	1.11	1.06	1.25	1.35	1.54	1.24	1.61	1.22
Moisture content %	10	13	12	11	8	9	8	8	9	11
Dry Density ( $g/cm^3$ )	1.12	0.96	0.99	0.95	1.16	1.24	1.43	1.15	1.47	1.10
<b>Lower Layer</b>										
Pit location (km)	<b>1.30</b>	<b>3</b>	<b>6</b>	<b>7.6</b>	<b>11.5</b>	<b>14</b>	<b>20.6</b>	<b>22.8</b>		
Bulk density ( $g/cm^3$ )	1.51	1.31	1.18	1.25	1.46	1.59	1.59	1.54		
Moisture content %	12	18	16	16	9	12	12	10		
Dry Density ( $g/cm^3$ )	1.35	1.10	1.01	1.08	1.34	1.43	1.42	1.40		

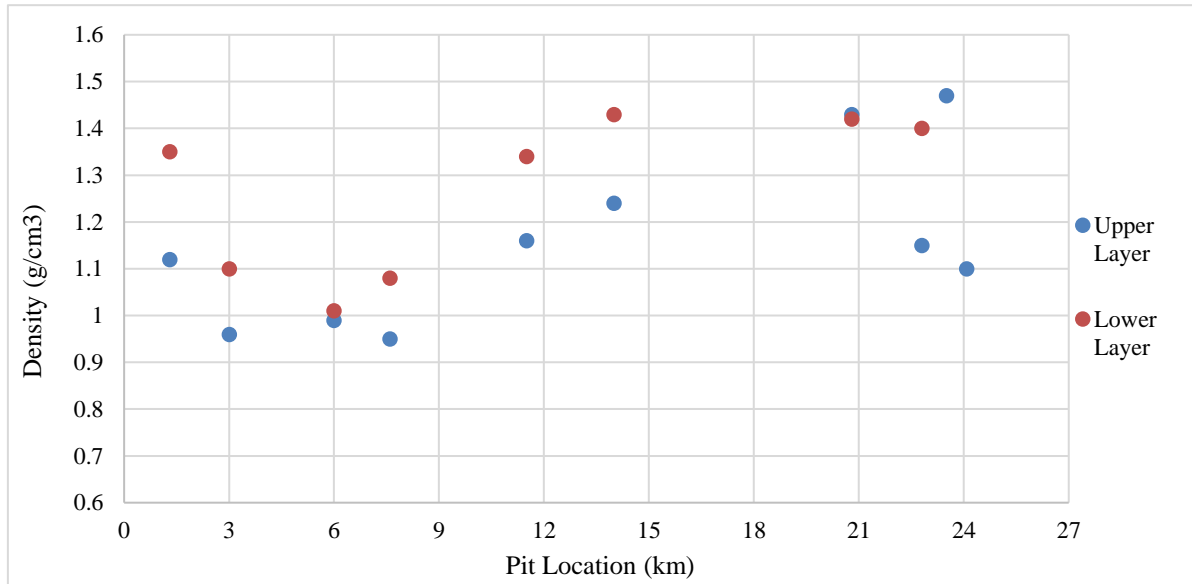


Figure 4-12: Dry Density of the Tested Pits

As seen from the test results dry density of the soil is low. The pyroclastic deposit inside of the rift valley (especially around the lake region) have low dry density value. For the majority of the stretch from Bulbula town up to station 14+000, the dry density value is below 1.3 g/cm<sup>3</sup>. On the section from station 14+000 to Alage, the dry density value is below 1.5 g/cm<sup>3</sup>. Comparison of field dry density and laboratory maximum dry density values is included in section 4.4.1.

When the volcanic emission cools down, it turns into solid rock. Since the rate of cooling is very fast during volcanic ash formation, crystal didn't form and has a lot of air mixed into it during the eruption, resulting in pockets of air trapped in the cooled-down rock. The air pockets and absence of crystals make volcanic ash lighter and have low dry density value.

### 4.3.2 Dynamic Cone Penetrometer

The primary data obtained from the DCP test are the number of hammer blows delivered and the corresponding depth of penetration, which directly gives the rate of penetration:

$$\text{Rate of Penetration}(DCPI) = \frac{\text{incremental penetreation in mm}}{\text{incremental blows}} \quad 4.2$$

The rate of penetration (in mm/blow units) is a good indicator of the stiffness of the material penetrated through and the relationship is inverse, i.e., the lower the rate of penetration, the higher is the stiffness of the material penetrated through and vice versus. The DCPI value obtained varies with depth, the weighted average DCPI value obtained in the test pits is

## Use of DCP and CBR tests to Characterize Subgrade Shear Strength

shown in Table 4-8 and Figure 4-13. Detailed analysis of DCP field data is included in the appendix of the report.

From station 14+000 to Alage the pyroclastic deposit is relatively strong. Approximately 80 cm below the existing ground level welded tuff was encountered at station 23+500 and 24+080 test pit locations.

**Table 4-8: Weighted Average DCPI Values**

<b>Upper Layer</b>										
Pit location (km)	<b>1.30</b>	<b>3</b>	<b>6</b>	<b>7.6</b>	<b>11.5</b>	<b>14</b>	<b>20.6</b>	<b>22.8</b>	<b>23.5</b>	<b>24.08</b>
DCPI (mm/blow)	30	18	17	21	42	13	6	15	16	19
<b>Lower Layer</b>										
Pit location (km)	<b>1.30</b>	<b>3</b>	<b>6</b>	<b>7.6</b>	<b>11.5</b>	<b>14</b>	<b>20.6</b>	<b>22.8</b>		
DCPI (mm/blow)	5	13	15	16	13	6	8	6		

The DCPI value generally provides more information about the strength and density of the material. As seen from visual site investigation and also confirmed by the DCP test results the majority section of the pyroclastic deposit up to station 14+000 is relatively loose than the deposit from station 14+000 to Alage.

In the past, the section from 14 km to 29 km was part of the Abiyata Lake. Even if there is no significant change in material type from 0 km to 14 km with that of 14 km to 29 km, as a result of the formerly Abiyata lake coverup in the second section, the pyroclastic material has a welded nature and is difficult to be penetrated by DCP probe. The load from Lake water provided densification to the pyroclastic deposit, this improved the density of the deposit and makes it difficult to be penetrated.

As it is indicated in section 4.2.6 the calcium and magnesium ion concentration from station 14+000 to 29+000 is higher than the section between station 0+000 to 14+000. When compared to the single charged cations of Sodium and Potassium, Calcium and Magnesium stabilize soil structure. This will also provide additional strength to the soil structure which will make it resistant to penetration of the DCP probe.

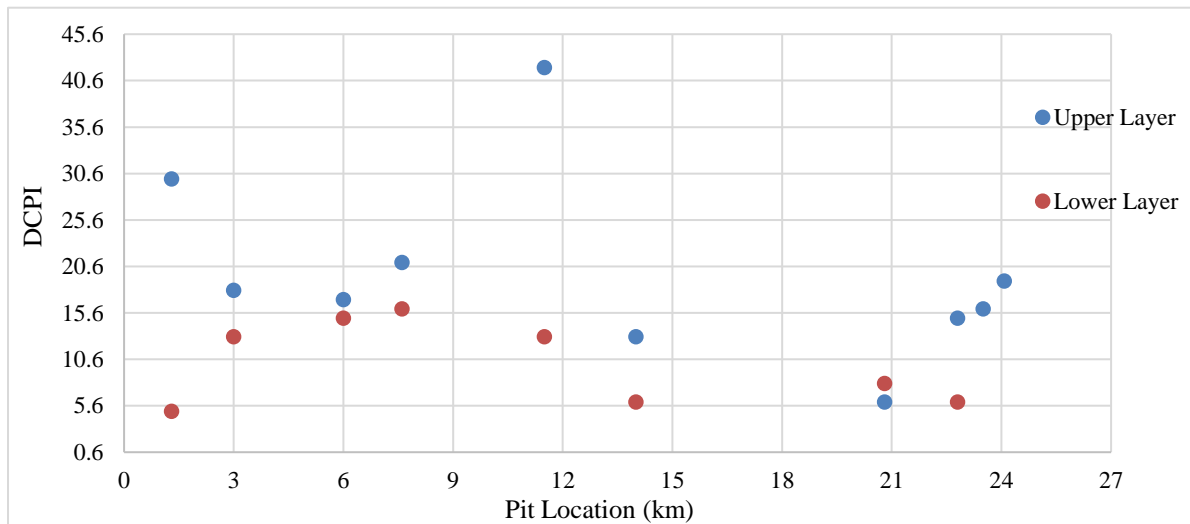


Figure 4-13: Rate of Penetration Value of the Tested Pits

#### 4.4 Comparison between Field and Laboratory Test Results

##### 4.4.1 Field and Laboratory Dry Densities and Moisture Content

Along the project route corridor in-situ density of the soil is lower than the maximum dry density (MDD) obtained in Laboratory. Since density value of the soil material is related with strength; under normal scenario existing strength value of the subgrade soil is expected to be lower than the one obtained in laboratory when molded to MDD.

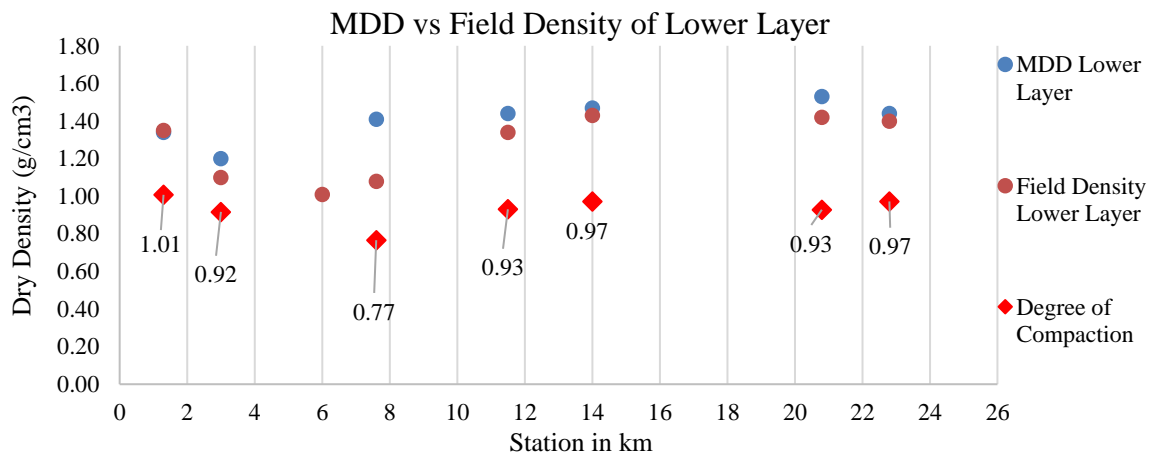
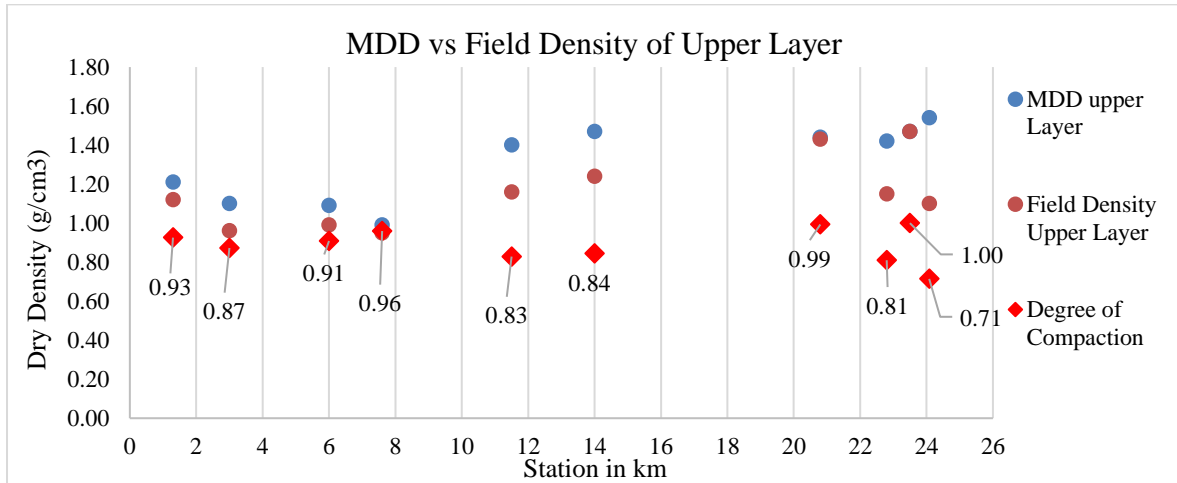
The average degree of compaction in the field when compared with laboratory MDD value in the upper layer is 88% and in the lower layer is 90%. Depth wise variation of test results is shown in Table 4-9 and Figure 4-14.

Table 4-9: Field and Laboratory Dry Density and Moisture Content Values

Station	Upper Layer				Lower Layer			
	Laboratory Test		Field Test		Laboratory Test		Field Test	
	OMC (%)	MDD (g/cm <sup>3</sup> )	Moisture (%)	Field Density (g/cm <sup>3</sup> )	OMC (%)	MDD (g/cm <sup>3</sup> )	Moisture (%)	Field Density (g/cm <sup>3</sup> )
1+300	26	1.21	10	1.12	21	1.34	12	1.35
3+000	20	1.10	13	0.96	22	1.20	18	1.1
6+000	28	1.09	12	0.99			16	1.01
7+600	37	0.99	11	0.95	19	1.41	16	1.08
11+500	20	1.40	8	1.16	24	1.44	9	1.34
14+000	22	1.47	9	1.24	21	1.47	12	1.43
20+600	23	1.44	8	1.43	22	1.53	12	1.42

## Use of DCP and CBR tests to Characterize Subgrade Shear Strength

22+800	24	1.42	8	1.15	24	1.44	10	1.4
23+500	25	1.47	9	1.47				
24+008	22	1.54	11	1.1				



**Figure 4-14: Laboratory MDD versus Field Dry Density values**

For the upper layer, the average of the laboratory maximum dry densities (MDD) is 1.31 gm/cm<sup>3</sup> while that of the In-situ dry densities is only 1.16 g/cm<sup>3</sup>, the average is 88% of laboratory MDD. For the lower layer average of the laboratory maximum dry densities (MDD) is 1.40 gm/cm<sup>3</sup> while that of the In-situ dry densities is only 1.27 g/cm<sup>3</sup>, the average is 90% of the laboratory MDD.

On the other hand, for the upper layer the in-situ moisture content is 10 % on average while the laboratory optimum moisture content (OMC) is 25 %. For the lower layer the in-situ

moisture content is 13 % on average while the laboratory optimum moisture content (OMC) is 22 %.

During direct shear testing to simulate realistic existing condition, the sample was remolded to attain field dry density value under the optimum moisture content (OMC). As the moisture content increases, the water lubricates the soil, allowing it to move more easily into a compact state and the density increases. At the optimum moisture content, the soil particles are lubricated very well that the required density was achieved easily. The DCP test undertaken in field was correlated with the angle of internal friction value obtained by remolding the soil sample to the field dry density value.

#### **4.4.2 CBR Value at Field and Laboratory Dry Densities**

Strength value of the soil is calculated at both field density and 95 % MDD. As shown in Table 4-10 and Figure 4-15. For the majority of the stretch CBR value at 95 % of MDD is higher than the one obtained at in-situ dry density.

Behavior of the soil change with depth, in order to identify the change in strength of the soil with depth, density and strength of the soil in the upper and lower depth have been examined. For the upper layer, the average of CBR value at 95 % of MDD (average of 95 % MDD = 1.24 g/cm<sup>3</sup>) is 24 % while at that of in-situ dry densities (average in-situ dry density = 1.16 g/cm<sup>3</sup>) is 16 %. For the lower layer, average of CBR value at 95 % of MDD (average of 95 % MDD = 1.33 g/cm<sup>3</sup>) is 37 % while at that of in-situ dry densities (average in-situ dry density = 1.27 g/cm<sup>3</sup>) is 32 %. In the pyroclastic deposit of pilot stretch section, with small increase in dry density value CBR of the material increases significantly.

**Table 4-10: CBR Value at MDD and Field Dry Density Values**

Station	Upper Layer		Lower Layer	
	CBR at 95% MDD	CBR at in Place Density	CBR at 95% MDD	CBR at in Place Density
1+300	8.5	7.7	34	47
3+000	34	21	36	20
6+000	17	14		
7+600	13.5	14	39	19
11+500	17	6.5	24	15
14+000	40	18	41	46
20+600	34	39	44	41
22+800	25	16	39	42
23+500	9	14		
24+080	37	10		

## Use of DCP and CBR tests to Characterize Subgrade Shear Strength

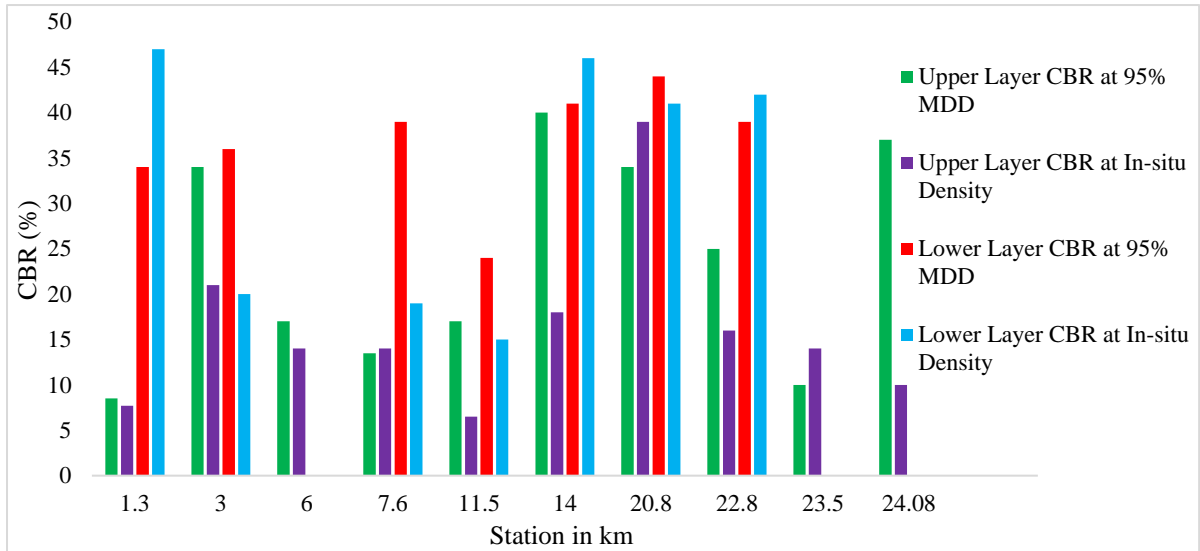


**Figure 4-15: Comparison of CBR Value at In-Situ Dry Density and 95% of MDD Value**

## CHAPTER 5      CORRELATION BETWEEN CBR/DCP AND SHEAR STRENGTH PARAMETERS

### 5.1 General

The existing manuals adopted in Ethiopia for road construction and management purpose have made CBR and/or DCP tests mandatory in order to characterize strength of unbounded materials. This situation made CBR and/or DCP test result data to be available easily for every road stretch throughout the country. Therefore, wherever you go one of the laboratory and field test results which will be easily re-claimed are CBR and DCP test results. Contrary to this the shear strength parameters which are used for slope stability analysis and bearing capacity computations are not available in sufficient number, due to this fact in majority circumstances the back and fore slope ratios presented in the manual are based on visual observation of material type.

The slope ratio table in ERA manual classified materials into five categories based on visual observation, this are: - earth soil, strong rock, weathered rock, decomposed rock and black cotton soil. Based on the type of material and height of the slope, slope ratio (vertical to horizontal) is provided. In the majority of circumstances, the geotechnical engineer involved in design and construction of road projects does not have shear strength parameters required for slope analysis purpose. Therefore, the geotechnical engineer simply took the recommended slope ratios of the manual based on visual observation of material type. But, the CBR and DCP tests are undertaken frequently during design and construction of road projects that, if these two tests are correlated with shear strength parameter, the data required for the analysis work will easily be available from the model.

In this research regression-based equations have been developed for shear strength value estimation with CBR and DCP values, as these tests are simply available due to the adopted road manuals of Ethiopia.

### 5.2 Regression Analysis

Regression analysis is a statistical method for relating a dependent variable to one or more independent (explanatory) variables. The variables are often designated as dependent or independent. A dependent variable, also known as an outcome, is impacted by an independent variable, which is an input. The dependent variable in this research is shear strength parameter. The independent variables are CBR and DCPI values.

The four main goals of regression analysis are description, estimation, prediction, and control. Regression can describe how dependent and independent variables relate to one another. Estimation is the process of determining the value of the dependent variable using the observed values of the independent variables. Based on the interactions between dependent and independent variables, regression analysis can be beneficial for forecasting outcomes and changes in dependent variables. The ability to control the impact of one or more independent variables while examining the relationship between one independent variable and the dependent variable is the final advantage of regression.

There are different kinds of regression analysis. Multiple regression models are regression models with several independent variables. Alternatively, regression model containing one independent variable is termed as simple regression model. Multiple regression makes the assumption that each independent variable does not strongly correlate with the others. Additionally, it presupposes that each independent variable and the sole dependent variable are correlated.

In a regression analysis the correlation coefficient ( $\rho$ ) determines the degree to which the movement of two different variables is associated. A scale from + 1 to -1 is used to calculate the correlation coefficient. Either + 1 or -1 represents a variable's complete connection with another. The most common correlation coefficient, generated by the Spearman's rho, is used to measure the non-linear relationship between two variables. It's a rank correlation coefficient because it uses the rankings of data from each variable (e.g., from lowest to highest) rather than the raw data itself. Equation 5.1 shows the equation of Spearman's rho correlation coefficient.

$$\rho(\text{correlation coefficient}) = 1 - \frac{6 \sum d_i^2}{n(n^2 - 1)} * 100 \quad 5.1$$

Were: -  $d_i$  = the difference between the x-variable rank and the y-variable rank for each pair of data

$\sum d_i^2$  = sum of the squared differences between x and y variable ranks

$n$  = sample size

During this thesis work, using regression analysis is used to relating CBR and DCP test results with that of angle of internal friction.

### 5.3 Correlation between DCP and CBR Values

Different correlations have been developed by researchers to convert the rate of penetration (DCPI) value into in-situ CBR strength. Especially UK DCP 3.1 software developed by transport research laboratory (TRL) have included more than seven correlations which are used to convert penetration rate into equivalent CBR value.

In this research the CBR value calculated at in-situ dry density was correlated with DCPI (penetration rate). During the investigation stage adjacent to the point where field density was determined DCP test was also undertaken. The sample taken for laboratory testing was retrieved from the same point where DCP and in-situ density tests were undertaken. Summary of correlation result between DCP and CBR test results is shown in Table 5-1.

**Table 5-1: Statistical Measure between DCPI and CBR Correlation**

<b>Correlations</b>		<b>Penetration Rate</b>	<b>CBR in %</b>
Spearman's rho	Penetration Rate	Correlation Coefficient	1.000
		Significance level	.
		Number of samples	18
	CBR in %	Correlation Coefficient	-0.963
		Significance level	.000
		Number of samples	17

The coefficient of correlation obtained between DCP and CBR test data is high that both data can't be used simultaneously for determination of shear strength parameters. The DCP and CBR tests are correlated negatively, when penetration rate increases CBR decreases and vice versus. And also, the significance level of correlation is below 0.05, this indicates a high level of correlation between penetration rate and CBR value.

If both are used simultaneously in predicting shear strength parameters it will result in multicollinearity. Multicollinearity is the occurrence of high intercorrelations among two or more independent variables in a multiple regression model. Multicollinearity can lead to misleading results when a researcher or analyst attempts to determine how well each independent variable can be used most effectively to predict or understand the dependent variable in a statistical model.

### 5.4 Modeling Shear Strength Parameters Using DCP or CBR Value

As seen from section 4.2.8, the cohesion value obtained from direct shear test is extremely low to none that it is technically feasible to ignore the cohesion obtained. Figure 4.1 also indicates the material along the route corridor is majorly none to low plastic. The material attains its strength from friction between intergranular particles.

The angle of internal friction is the significant and major contributing factor for strength of the pyroclastic deposit of the route corridor that it will be correlated with DCPI and/or CBR values obtained. The CBR value calculated at in-situ density and the DCPI value obtained from field test have been used for this correlation or modeling purpose. The correlation developed have been undertaken using Excel spreadsheet and SPSS statistical analysis software.

$$\phi \text{ (in degree)} = 52.676 - 7.749 \ln(\text{DCPI}); R^2 = 0.9449 \tag{5.1}$$

$$\phi \text{ (in degree)} = 16.458 * \text{CBR}^{0.2269}; R^2 = 0.835 \tag{5.2}$$

The coefficient of determination value obtained between  $\phi$  and DCP correlation is higher than that of  $\phi$  and CBR correlation. The scatter plot obtained is shown in Figure 5-1 and 5-2.

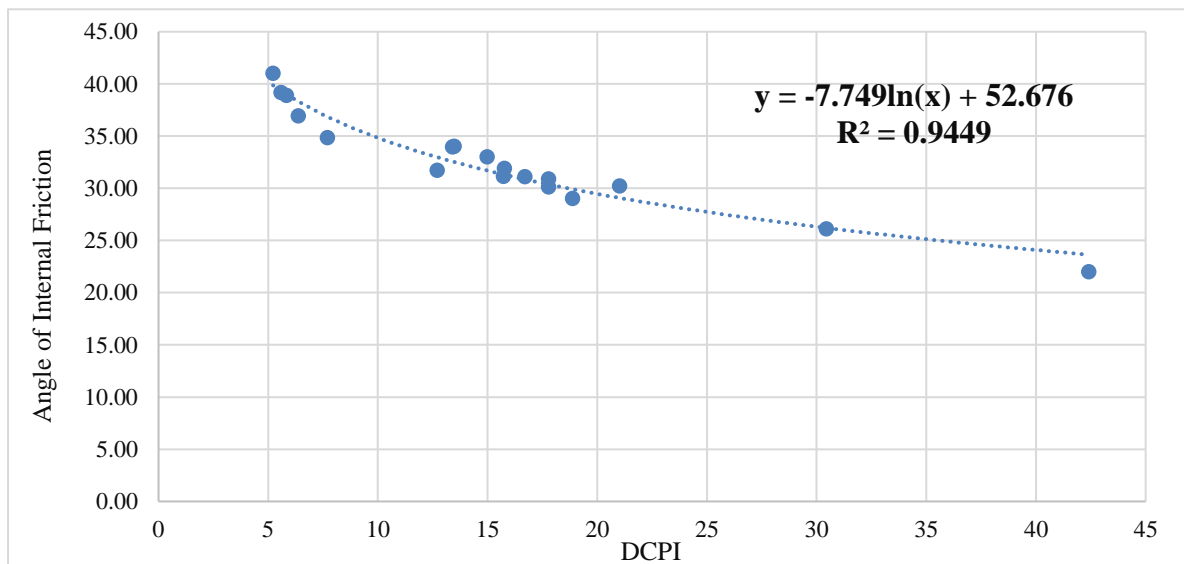


Figure 5-1: Correlation/Scatter Plot Between Angle of Internal Friction and DCPI Values

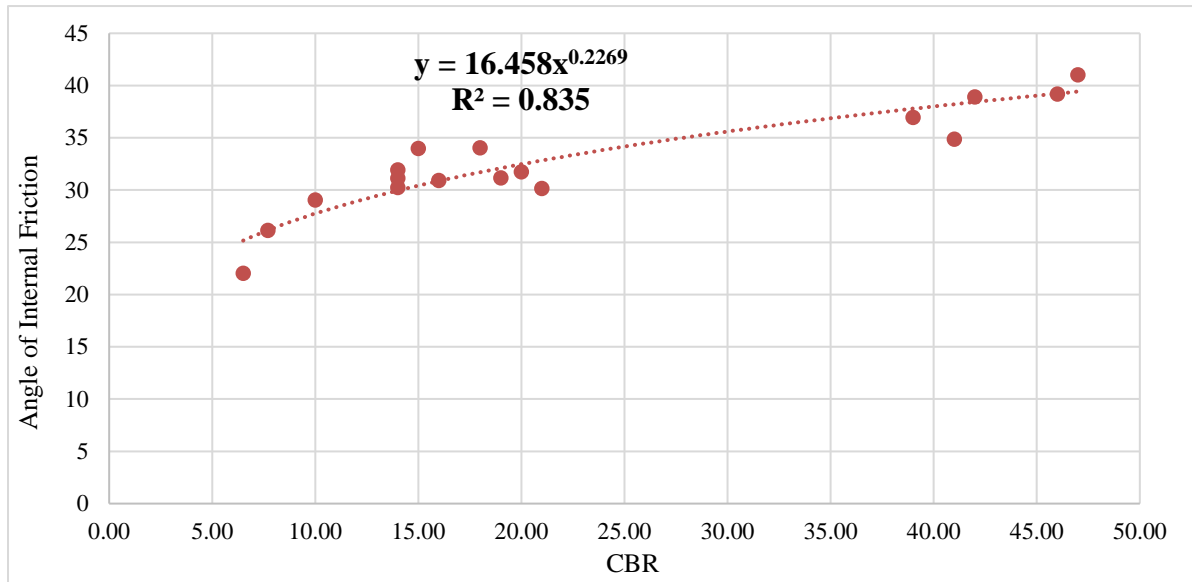


Figure 5-2: Correlation/Scatter Plot Between Angle of Internal Friction and DCPI Values

Table 5-2: Statistical Summary for the Correlation

Angle of Internal Friction and DCPI				
R	R Square	Adjusted R Square	Std. Error of the Estimate	Significance Level
0.972	0.945	0.941	1.128	0.000
Angle of Internal Friction and CBR				
R	R Square	Adjusted R Square	Std. Error of the Estimate	Significance Level
0.914	0.835	0.824	0.064	0.000

A summary of the statistical analysis result is shown in Table 5-2. The correlation coefficient value obtained is very high that the model developed is strong. Standard error of the estimate which is a measure of the average deviation of the errors, the difference between the values predicted by the model and the values in the sample is low that it also indicates the developed model is strong. The significance level/P-value in both correlations is very low that there is strong correlation between CBR and/or DCPI with that of angle of internal friction.

## CHAPTER 6 CONCLUSION AND RECOMMENDATION

### 6.1 Conclusion

Based upon the existing reality of Bulbula – Alage pilot stretch area and test result analysis, the following conclusions can be drawn:

- In majority sections of the route corridor dry density and strength values of the deposit increases depth wise.
- In majority section of the route corridor in-situ dry density value is lower than the MDD value
- The DCP and CBR tests are highly correlated that both data can't be used simultaneously for determination of shear strength parameters. Because if both are used simultaneously in predicting shear strength parameters it will result in multicollinearity.
- Dry density value obtained in both laboratory and in-situ tests indicates, the maximum dry density is mainly below  $1.5 \text{ g/cm}^3$
- The pyroclastic deposit along the route corridor has low to none plasticity
- The proportion of sand size particles in the soil is significant
- Even if the dry density value is low CBR value is high. The pyroclastic deposit has low CBR swell value
- The direct shear test result indicates the soil attain its strength from friction between materials
- DCPI value obtained indicates strength of the soil increases depth wise.
- Dispersive soil identification tests indicate the subgrade material belongs to non-dispersive to moderately dispersive class.
- The sodium and potassium ion concentration in the soil from station 0+000 to 15+000 is higher than that of station 15+000 to 29+000. The calcium and magnesium ion concentration in the soil from station 0+000 to 15+000 is lower than that of station 15+000 to 29+000. Calcium and magnesium stabilize soil structure, the calcium that is adsorbed to soil particles helps in stabilizing the soil structure. In-situ strength of the soil from station 15+000 to 29+000 is relatively higher than station 0+000 to 15+000 soil.
- The one-dimensional collapse potential test indicates the soil is moderately collapsible

- For the none to low plastic, low dry density, high CBR and moderately collapsible potential soils/pyroclastic deposited materials; the angle of internal friction can be reasonable estimated from CBR or DCP test result.
- The coefficient of determination value obtained on the correlation of  $\phi$  and DCP is higher than the one obtained between  $\phi$  and CBR correlation.

### 6.2 Recommendation

- The shear strength test was undertaken by remolding the disturbed sample to in-situ dry density state. Attempts shall be made to bring undisturbed pyroclastic deposit sample and compare results of remolded and undisturbed samples direct shear test results.
- The maximum sampling depths of the soil under investigations were 1.6 m. In order to deeply understand behavior of the pyroclastic deposit depth wise, samples shall be retrieved from deeper depths and be tested.
- The shear strength test was undertaken by direct shear test which has a predetermined failure plane. Undisturbed samples of the deposit shall be tested with both direct shear and triaxial tests in order to quantify the variance between the two testing methods.
- If shear strength parameters are estimated with available test results, the geotechnical engineers involved in road design and construction works will have an input value which will be used for slope stability analysis. This will encourage the professionals to undertake slope stability analysis instead of using presumed values. Therefore, additional correlations for other subgrade material types shall be developed.

## REFERENCES

- AASHTO. (2001). *American Association of state highway and transportation officials*. Washington: American Association of state highway and transportation officials.
- Alexander, B., et al. (2020). The 1951 eruption of Mount Lamington, Papua New Guinea: Devastating directed blast triggered by small-scale edifice failure. *Journal of Volcanology and Geothermal Research*, pp. 8-10.
- Anteneh, G. (2012). *Correlating Dynamic Cone Penetration Index (DCPI) with Undrained Shear Strength for Clayey Soils*. Addis Ababa: Addis Ababa University.
- Arora, K.R. (2004). *Soil Mechanics and Foundation Engineering*. Delhi: A.K.Jain.
- ASTM. (2015). *Standard Test Method for Use of the Dynamic Cone Penetrometer in Shallow Pavement Applications*. West Conshohocken: ASTM International.
- Black, W. (1979). *The Strength of Clay Subgrades: It's Measurement by a Penetrometer*. Crowthorne, Berkshire, UK: Transport and Road Research Laboratory.
- Bolt, G.H, and M.G.M Bruggenwert. (1978). Soil Chemistry: A. Basic Elements. Second rev. *Elsevier Scientific Publishing* .
- Elges, H. (1985). Dispersive soils. *The Civil Engineer in South Africa*, 347-353.
- ERA. (2013). *Site Investigation Manual* . Addis Ababa: Ethiopian Road Administration .
- Esposito, L., and Guadagno, F.M. (1998). Some Special Geotechnical Properties of Pumice Deposit. *Bull Eng Geol Env* 57, 41-50.
- Fisher, R.V., and Schmincke, H.U. (1984). *Pyroclastic Rock*. Berlin, Heidelberg, New York, Tokyo: Springer-Verlag.
- Gondwana Engineering. (2018). *Modjo - Hawassa Express Road Project Lot-3, Ziway (Batu) – Arsi Negele Section*. Addis Ababa: SBI International Holding AG (Ethiopia Branch).
- Gregory, G., and Cross, S. (2007). *Correlation of CBR with Shear Strength Parameters*. Stillwater, Oklahoma: Transportation Research Record, Vol. 1989, Issue. 1.

- Hogentogler, J.R. (1936). Essentials of Soil Compaction. *In Proceedings of the Sixteenth Annual Meeting of the Highway Research Board*, 309 - 316.
- Jacopo, T., and Danilo. M.P. (2002). Particle Size-Density Relationships in Pyroclastic Deposits: Inferences for Emplacement Process. *Bull Volcanol* (2002) 64, 273–284.
- Jennings, J. E., and K. Knight. (1975). A Guide to Construction on or With Material Exhibiting Additional Settlement Due to Collapse of Grain Structure . *Journal of Soil Mechanics and Foundation Engineering, 6th Regional Conference for Africa on Soil Mechanics and Foundation Engineering*,, 99-105.
- Katie, K. (2019). *Association of Geotechnical and Geoenvironment Specialists*. Retrieved from AGS: <https://www.ags.org.uk/2019/09/safety-and-technical-concerns-of-using-a-dcp/>
- Krishna, R. (2002). *Engineering Properties of Soils Based on Laboratory Testing*. Chicago: University of Illinois at Chicago.
- M.Das, B. (1997). *Advanced Soil Mechanics*. London: Taylor & Francis.
- Manuela, C., et al. (2009). On the Geology and the Geotechnical Properties of Pyroclastic Flow Deposits of the Colli Albani. *Bull Eng Geol Environ*.
- Mengesha, T., et al. (1996). *Geological Map of Ethiopia*. Addis Ababa: Ethiopia Institute of Geological Survey.
- Mohr, P.A. (1966). *Tectonic Map of the Afar-Plateau Boundary in Wollo and Tigris*. Addis Ababa: Addis Ababa University.
- Muni, B. (2006). *Soil Mechanics and Foundations*. Arizona: University of Arizona.
- Parveen, A., and Ahtisham, Y. (2021). *Understanding and Interpreting Regression Analysis*. Sheffield: Sheffield University.
- Purwana, M., and Nikraz, H. (2014). The Correlation between the CBR and Shear Strength in Unsaturated Soil Conditions. *International Journal of Transportation Engineering*, Vol. 1, No.3.

- Simon, D., and Piouslin, S. (2006). *Measuring Road Pavement Strength and Designing Low Volume Sealed Roads using the Dynamic Cone Penetrometer*. Berkshire: TRL Limited.
- Tam, B., and Dave, J. (1993). *In Situ Foundation Characterization Using the Dynamic Cone Penetrometer*. Minnesota: Minnesota Department of Transportation.
- Temnit, F. (2014). *Determination of Unconfined Compressive Strength (UCS) from Dynamic Cone Penetrometer Index(DCPI) for Red Clay Soil of Addis Ababa*. Addis Ababa: Addis Ababa University.
- Walker, G.P.L., and Croasdale, R. (1971). Characteristics of Some Basaltic Pyroclastics. *Bull. Volcanol*, 303-317.
- Woldechirkos, Y. (2016). *Application of Dispersive Soils as a Sub-Grade and Embankment Materials*. Addis Ababa: Addis Ababa University.
- Woldechirkos, Y., and Desaleg, K. (2020). *Soil and Material Investigation Report*. Addis Ababa: Sound Consulting Engineer plc.
- Woldegabriel, G., et al. (1990). Geology, Geochronology, and Rift Basin Development in the Central Sector of the Main Ethiopian Rift. *Geological Society of America Bulletin*, pp. 439-458.
- Yitagesu, D. (2012). *Developing Correlation Between DCP and CBR for Locally Used Sub Grade Materials*. Addis Ababa: Addis Ababa University.

**APPENDIX**